

Aus der Klinische Neurobiologie des Universitätsklinikums und DKFZ  
(Direktorin: Prof. Dr. Hannah Monyer)

# Context-specificity of spatially selective neurons in the medial entorhinal cortex

Inauguraldissertation

zur Erlangung des *Doctor scientiarum humanarum (Dr. sc. hum.)*

an der

Medizinischen Fakultät Heidelberg

Der

Ruprecht-Karls-Universität

vorgelegt von

*José Antonio Pérez Escobar*

Aus

*Almeria, Spanien*

2023

Dekan: Prof. Dr. med. Hans-Georg Kräusslich  
Doktormutter: Prof. Dr. med. Hannah Monyer

<b>Contents</b>	<b>Page</b>
<b>1. Introduction</b> .....	5
1.1 Spatial navigation .....	6
1.2 The cognitive approach to spatial navigation .....	8
1.3 The neurobiological substrata of spatial navigation .....	14
1.3.1 Place cells .....	15
1.3.2 Head-direction cells .....	15
1.3.3 Border cells .....	16
1.3.4 Speed cells .....	16
1.3.5 Grid cells .....	17
1.4 Aim of the study .....	18
<b>2. Materials and Methods</b> .....	19
2.1 Surgical procedure .....	19
2.2 Recording system, spike extraction and spike clustering .....	20
2.3 Initial training .....	21
2.4 Circular arena .....	21
2.5 Identification of spatially selective neurons .....	23
2.6 Stability of firing rate maps .....	26
2.7 Spike distance metric .....	26
2.8 Distance coding by grid cells .....	27
2.9 Detection of putative excitatory connections .....	27
2.10 Linear track experiment .....	28
2.11 Linear firing rate maps .....	29
2.12 Histology .....	30
<b>3. Results</b> .....	30
3.1 Circular arena experiment: broad effects of lack of visual information on spatially selective MEC neurons .....	30
3.1.1 Visual landmarks anchor MEC spatial representations .....	32

3.1.2 Rapid degradation of grid cell periodicity in absence of visual landmarks .....	32
3.1.3 Partly preserved distance coding by grid cells in darkness .....	35
3.1.4 Influence of visual information on speed coding in the MEC .....	37
3.1.5 Impaired border representation in darkness .....	41
3.1.6 Reduced head-direction selectivity in darkness .....	42
3.1.7 Firing rate changes in MEC neurons between light and dark trials .....	43
3.2 Linear track experiment: Firing rate changes associated with nonmetric contextual cue manipulation in 1D environment .....	46
<b>4. Discussion</b> .....	50
4.1 Effects of the removal of visual input on spatially selective cells in the MEC .....	50
4.2 Heterogeneous information encoding .....	52
4.3 Research building on the effects of visual landmarks and context-specificity of grid cell activity shown in this work .....	54
4.4 Path integration and representationalism .....	56
4.5 Alternative takes on representations .....	57
<b>5. Summary</b> .....	61
<b>6. Zusammenfassung</b> .....	62
<b>7. References</b> .....	63
<b>8. Publications</b> .....	77
<b>Acknowledgements</b> .....	78
<b>Affidavit</b> .....	80

# 1. INTRODUCTION

The neuroscience of spatial cognition is a very heated field of research today. The reasons for this are numerous and varied, and among them there are the following two:

-It has been an important catalyzer for the import of mathematical and computational techniques to address the so-called higher cognitive functions. The methodological challenges that brought cognitive science apart from cognitive neuroscience in the 1990s<sup>1</sup> (Kriegeskorte and Douglas, 2018) have been partially resolved. This resolution has led – and continues to lead – to important insights on how brain systems perform cognitively relevant computations. Therefore, the field is reinvigorating the hopes of those seeking a synthesis of cognitive science, neuroscience and even engineering and computer science.

-The award of the 2014 Nobel Prize in Physiology or Medicine to John O’Keefe, Edvard Moser and May-Britt Moser for the characterization of place cells and grid cells, prominent neuronal substrata of spatial cognition, has only but aggrandized the field and promoted the already substantial attention paid to it.

These two pieces of the recent story of the neuroscience of spatial cognition are reasons for excitement, which is much needed to overcome further theoretical, technical and methodological problems. However, it should be acknowledged how challenging representation/information and function ascription is in cognitive neuroscience, as I will try to show in this work. What follows is a segmented introduction to spatial behavior, spatial cognition, their neurobiological substrates, and the main challenge

---

<sup>1</sup> Cognitive science usually follows a top-bottom approach, while cognitive neuroscience favors a bottom-top approach. Cognitive science built “boxes and arrows” models of cognition in its effort to elaborate useful descriptions of higher cognitive functions. Cognitive neuroscience, on the other hand, while tolerating this approach and trying to map the boxes’ cognitive modules onto the brain, suffered in terms of computational rigor and neurobiological plausibility, finally resulting in the two disciplines parting ways.

that this work intends to note and address: the complex and equivocal character of the relation among 1) material substrata, 2) cognition/information, and 3) function.

## 1.1 Spatial navigation

Spatial navigation is considered a key ability for survival in many organisms, from small and relatively simple insects to complex mammals like primates and humans. Therefore, it is a basic behavioral function. The function is ubiquitous in the animal kingdom. It is crucial for prey seeking/predator avoidance, foraging, returning to safe environments, hiding food for winter, pollinating flowers, and much more. In fact, given the evolutive importance of spatial navigation, one could infer the existence of shared or similar mechanisms in classes of organisms that share sizeable portions of recent evolutive paths – like complex mammals, or certain insects. Insects (perhaps the most studied are bees and ants) must forage and return to a starting or reference point (the colony, the nest, the hive) for survival, and they seem to share common mechanisms that put them in a different class to that of mammals (Collett et al, 2013). In this work, nonetheless, when describing the neurobiological substrata of spatial navigation, the focus resides on mammals: the so-called “mammal brain” is a generality based on the notion that mammals display significant brain structure similarity across species.

Spatial navigation has been more studied, documented and characterized in mammals than in any other class (in the taxonomic rank sense). There are several reasons for this. The most obvious one is that humans belong in the class “mammals”, and the hopes of finding connections between basic and applied science are bigger here. A bit of speculation leads to other reasons. It may be easier to perform finer experiments and isolate relevant variables with mammals. Maybe their cognition is more complex and interesting as a whole to the eyes of scientists: spatial navigation is linked to cognitive abilities like memory (spatial working, short-term and long-term memory, visual memory, object memory...), after all, and spatial navigation could be a bridge to the

understanding of higher cognition. Be the reasons anthropocentric, technical or utilitarian, it is this way and it shows. For instance, there are many standardized experimental procedures to study spatial navigation in rodents: paradigmatic experimental settings such as the radial maze (Olton and Samuelson, 1976) and the Morris water maze (Morris, 1981), virtual reality settings, and so forth. There is also a substantial amount of human experimentation, such as taxi/bus driver experiments (for instance, Maguire et al., 2000; Maguire et al., 2006), virtual reality/videogame based experiments, etc.

Spatial navigation has been characterized as a process that relies on both allothetic and idiothetic information. Allothetic information is about environmental cues outside the organism itself (for instance, visual, auditory, olfactory, and tactile cues/landmarks, and environmental geometry) that act as spatial references. An illustrative example is sailors using the position of the stars to navigate the sea. On the other hand, idiothetic – or internal – information refers to information related to the subject, which is mostly derived from self-motion, and includes vestibular, proprioceptive, motor efference copy and optic flow information (Poulter et al., 2018), and can also act as spatial reference. In fact, they can be experimentally dissociated, for example in virtual reality (Tennant et al., 2018). Both types of information complement each other, and their mismatch leads to confusion. In such situation, or when one type of information is absent, the organism may adopt allocentric or egocentric navigation strategies, depending on whether it predominantly relies on allothetic or idiothetic information respectively. In the specific situation that allocentric information is completely or for the most part absent (or disregarded due to incoherency), many species resort to a navigational strategy termed “path integration” which consists on the vector calculation of a return path after venturing away from a starting position (Jander, 1957; Görner, 1958; Mittelstaedt and Mittelstaedt, 1980; Müller and Wehner, 1988).

Prolongued reliance on path integration and absence of allothetic information leads to cumulative error over time. An organism can try to orientate in space in the absence of allothetic information (darkness, silence, no smells, no tactile cues) with certain degree of precision, but eventually the accumulated error will make it inefficient to

perform the spatial navigation task in question. Valerio and Taube (2012), for instance, found that both the length of the outward trip and the number of head turns are associated with a higher error probability when rats path-integrate and return to a reference point. This suggests that the more traveled distance and head turns need to be integrated, the more error is accumulated.

However, I mentioned before that allothetic and idiothetic information are complementary, and the sudden or increased availability of the former can help correct cumulative error during path integration (Ethienne et al., 1996; Ethienne et al., 2000; Ethienne et al., 2004). It is proposed that the path integrator can be reset by just establishing minimal contact with environmental boundaries, since it realigns grid cell activity (Hardcastle et al., 2015), which as we will see, is the proposed neurobiological substratum of path integration. In fact, environmental boundaries seem to exert a deep and more generalized influence on grid cell activity, like on its orientation, scaling and hexagonality (Stensola et al., 2012; Krupic et al., 2015; Krupic et al., 2018).

## **1.2 The cognitive approach to spatial behavior**

Even if one could start from a much earlier point in history, for the purposes of this introduction this story begins with the transition from behaviorism, one of the most prominent schools of thought in psychology during the first half of the 20<sup>th</sup> century, to cognitivism. Cognitive neuroscience, after all, presupposes and is based on many postulates of cognitivism. Therefore, I will not present here an overview of different accounts of behavior and the mind in general, or spatial navigation in particular. Instead, I will restrict the theoretical background to the cognitive turn (more often called “cognitive revolution”) and the cognitive approach to spatial behavior.

I mentioned before the link between spatial navigation and higher cognition as a potential source of interest and motivation for researchers to study spatial navigation in mammals. This link entails bold metaphysical assumptions, at least as many as

cognitivism itself (of which the most prominent are perhaps ontological commitments to mental representations and a causal direction from mind to behavior).<sup>2</sup>

Cognitive neuroscience and, by extension, computational neuroscience,<sup>3</sup> are framed by the postulates of cognitivism. In order to better understand the difficulties and endeavors of the field, it is important to make them explicit. A precise and encompassing account of cognitivism falls out of the scope of this work, and hence not much space can be dedicated to it. However, the following quotes by Gerrans (2014) are illustrative of my simplified overview: 1) cognitive neuroscience conceives “persons as complex, hierarchically-organized information processing systems implemented in neural wetware” (p. 16), 2) the mind in such neural wetware “uses representations of the world and its own states to control behaviour” (p. 47). Furthermore, and to the dismay of many anthropologists, some degree of universality seems to be endorsed by cognitivist approaches, as psychologist Steven Pinker (2002) argues: one of the key ideas that defined the cognitive revolution is the existence of “universal mental mechanisms can underlie superficial variation across cultures” (p. 37). Miller and Chomsky, two of the figures responsible for crafting the snowball which would become the cognitive revolution, propose paradigmatic examples of this idea in the form of “the magical number seven, plus or minus two: some limits on our capacity for processing information” and universal grammar<sup>4</sup> respectively (Miller, 1956; Chomsky, 1955/1956; published 1975; Chomsky, 1959; Chomsky, 1962).

---

<sup>2</sup> This is not to say that alternatives do not entail metaphysical assumptions, axioms, ungrounded ground premises and basically starting points that cannot ultimately be in turn justified by a ground of grounds. The reasons to adhere to some accounts or frameworks over others (say, cognitivism over behaviorism), or to some subaccounts over others (say, varieties of computationalism and functionalism), even if sometimes foreclosed under the guise of common sense or epistemological virtue, have an important pragmatic dimension.

<sup>3</sup> Strictly speaking, computational approaches and in general the logic of information processing do not necessarily entail cognitivism (see, for instance, Copeland and Shagrir, 2013). Still, in practice, computational neuroscience is usually understood as a subdiscipline of cognitive neuroscience. Therefore, likely due to the current dominance of cognitivism, computational neuroscience is cognitively framed. However, the inverse does not apply: it is commonly accepted that not all accounts of cognition are computational. The result is that, while in principle none of the two disciplines must entail each other, computational neuroscience is understood and practiced as a subtype of cognitive neuroscience: all computational neuroscience is cognitivist but not all cognitive neuroscience is computational.

<sup>4</sup> Chomsky’s idea of universal grammar purports to explain the generation of sentences in daily life by appealing to inner and innate transformation rules, and is inspired by the languages of the at the time incipient field of computer science.

Today, spatial navigation is studied via the uncontested, foreclosed lens of a cognitivist framework. But this not the only framework possible and certainly not the only one that has been applied to spatial navigation. Behaviorism was one of these frameworks. The classical example of behavioral account of spatial navigation (but also problem solving more broadly) is Thorndike's work on cats finding their way out of puzzle boxes, leading to his Law of Effect: stimulus-response (S-R) associations are reinforced if they bring about "satisfactory" outcomes, and complex behaviors are concatenations of S-R associations the apprehension of which is subjected to gradual learning via trial and error (Thorndike, 1898; Thorndike, 1905).

The seminal work leading to a cognitive framing of spatial behavior came from the hand of Tolman in the form of the cognitive map theory. Consistently with Kant's epistemology<sup>5</sup> but never acknowledging him, he claimed that rat's and men's spatial behavior cannot be explained by mere S-R associations. For example, when standard or familiar routes are unavailable, rats can reach a goal navigating alternative paths in absence of previous direct experience with them (Tolman et al., 1946a; Tolman et al., 1946b). An internal representation of space may, however, govern complex spatial behaviors like this, both in rats and humans (Tolman, 1948). Thus, Tolman's work initiated a shift from a behaviorist account of spatial behavior to a cognitivist one: the complexity of spatial behavior cannot be explained by reinforcement-based learning; instead, there is a mental representation which *causally* accounts for spatial behavior.

---

<sup>5</sup> The most commonly accepted historical sketch is the following: Kant offers in his critiques a synthetic alternative to Cartesian (series of logical inferences/deductions based on self-evident premises) and Humean (the rejection of a rationalist model based on sufficiently reliable premises and rules of deduction, and the proposal of empirical observation as the foundation of knowledge) epistemologies. Kant thus proposes two dichotomies, *a priori* - *a posteriori*, and analytic - synthetic. The *a priori* is independent of experience, and the *a posteriori* is based on experience. The analytic does not add knowledge beyond the content present within its own concepts and premises (the cat is a mammal), while the synthetic does (the cat is brown). Kant concedes to Descartes that we can create knowledge without observing (synthetic - *a priori*), as when doing mathematics or metaphysics, but he also concedes to Hume that observation is critical for all other types of knowledge. Of course, now that knowledge does not depend exclusively on the Cartesian method (logical inferences) or mere observation (raw input from the senses), there is an epistemic subject that plays a key role in intelligibility, in creating and ordering knowledge. The Kantian version is that this epistemic subject has two basic *a priori* forms of sensible intuition which frame the world: time and space. Cognitivists usually put forward notions similar to such *a priori* forms, but Tolman's cognitive map theory is a special case because it fits one of the two Kantian pure forms of intuition.

Endorsing Tolman's cognitive theory of spatial behavior has two substantial consequences. The first is that a departure from associative learning entails, in turn, a departure from neural learning processes grounding it (or at least, the need to build on them to accommodate representations and information processing). The second is that a cognitive representation of space is such a broad concept that is of little use if it is not further decomposed. For instance, for an animal to perform efficient spatial behavior, it must represent the metric characteristics of the environment, allothetic environmental cues, its position within it, its moving direction, its speed, and so forth. Furthermore, there must be neurobiological substrata responsible for these representations, and the understanding of such substrata may further clarify the representations and the manner in which information is processed (note the epistemic circularity involved).

All in all, the task of cognitive neuroscience is to answer the following question: which biological substrates sustains which representations, which causally account for which behavior more or less universally across organisms of the same species?

I cannot overstate the magnitude of this apparently simple "pairing" task. I will only sketch three difficulties:

- 1) Although the quest to find the neurobiological substratum of something seems to suggest a pairing process, we cannot forget there are actually three levels at stake: neurobiology, cognition (representations/information) and behavior. It does not suffice with pairing neurobiology and representations, or neurobiology with behavior, or representations with behavior. This sounds obvious but its implications are usually not so in practice. For instance, from the fact that a neurobiological substratum is involved in some behavior (for example, the behavior may be disrupted after the inactivation of the substratum in question), it does not follow that such a substratum represents a specific content related to such behavior, but intuitively, one could be tempted to establish such link.

2) It is especially problematic to ascertain the character of the supposed representations emerging from neurological substrata. The failure of phrenology is widely known, and leaves much room for improvement. However, the metaphysical assumptions of cognitivism, and the fact that the mapping is supposed to link two very distinct realms – the material and the mental – suggest that it is possible that improvement may come only in degrees. I will not review here the literature about the possibility of explanatory models establishing causality from matter to mind. I will briefly note that:

- Specific forms of mental representation are inferred from both neurobiological bases and behavior, not obtained as a material product. Causal links between neurological bases and behavior (matter – matter, or mechanism) are less problematic, while mental representations are convenient ontologies that fill the explanatory gap between the two – hence the causal direction from cognition to behavior of cognitivism. Being non-material, however, their precise formulation enjoys plenty of elbowroom, and takes the form that better fits the explanatory gap in a given practical context. Because of this, these ontologies are usually inspired by familiar material objects and concepts (computers, maps, compasses, speedometers, vectors, computation...).

- Gradual improvement may be a matter of fine-tuning correlations between the neurobiological substrata and the representation. Raichle (2009) presents a historical sketch of brain-mind mapping that fits a picture of progressive fine-tuning, starting with Italian psychologist Angelo Mosso noting a correlation between mathematical calculations and increased brain blood flow (obviously, a lack of blood flow would hinder the ability to perform mathematical calculations –manifested verbally, or via pen and paper). From this fact it does not follow, however, that from blood flow a mind emerges, and especially not concrete mental ontologies (e.g. abstract mathematical objects).

- Progress in cognitive neuroscience may also be a matter of fine-tuning the specific cognitive ontologies in the much pragmatic and instrumentalist sense that they better assist with filling explanatory gaps. In this line, it should be

noted that the theoretical construct of cognitive maps itself has been called into question (Bennett et al., 1996). Perhaps, eventually something better than an improvement that comes in degrees will be achieved by filling matter-matter explanatory gaps, discarding cognitivism altogether, and leading to yet another paradigm. Without advocating the latter radical scientific revolution, part of the discussion on the experimental results in this dissertation commits to this pragmatic view of cognitive representations.

3) There is some degree of epistemic circularity in the process. Certain behaviors are intuitively explained by a cognitivist framework. We choose to commit to the Kantian spatial *a priori*, a certain causal directionality, representationalism, and specific representational forms assisted by references to material observables (here, neurobiological and behavioral) that only underdetermine abstract ontologies. Then, these abstract ontologies become in turn the reference to investigate the neurobiological bases and overt behavior. And again, in turn, this investigation fine-tunes the representations to which we commit. This process works in a never-ending loop without a certain starting point: historically, did the observation of behavior lead to the idea that a mind causes it? Or did mental intuitions precede the observation of behavior? Probably this is not the right way to look at an issue that is subjected to such a co-production of the elements involved. More importantly, there is no ending point either. As Quine famously showed some decades ago, metaphysical notions and theoretical frameworks in general inevitably frame empirical observations (Quine, 1951); therefore, there is no such thing as neutral observations of nature, observations a neutral standpoint. Hence, empirical observations cannot be used to put metaphysics to the test. The point is then not to ground metaphysics in *physis* (nature), an enterprise which has been shown time and again to be deceptive and misleading. The point is not to reach the “real” abstract representations of nature (or even to determine whether these exist in a metaphysically strong sense). The point is to build a coherent, harmonical picture that puts cognitivism and its metaphysical postulates to work together with neurobiological and behavioral knowledge, in a way that is optimized for each scientific practice. In fact, this very task forecloses the issue of whether there are causally active representations arising from matter: it is a framework, an axiom of

the approach, a bedrock belief, a Wittgensteinian hinge proposition on which the rest builds, not something to be ascertained.

In this section I have tried to provide some context about the tasks of cognitive neuroscience. In addition, I have sketched some of the most prominent challenges. All in all, if we decide to commit to cognitivism, we need to bear in mind that cells, cell networks or brain structures, regardless of their behavioral functions, may not straightforwardly align with representation and information concepts that, for one reason or another, are intuitive to us. Now that the complicated picture has been sketched, I will briefly present the neuronal bases of spatial representations and behavior, with an emphasis on grid cells in the medial entorhinal cortex (MEC).

## **1.3 The neurobiological substrata of spatial navigation**

### **1.3.1 Place cells**

An early observation in rats showed that some hippocampal cells selectively fire when the animal is in a given region of the environment (O'Keefe and Dostrovsky, 1971). A few years later, O'Keefe recorded cells from the cornu ammonis region 1 (CA1) and coined the term "place units" to name neurons the activity of which is tuned to the animal's presence in a specific region of the environment (O'Keefe, 1976). These results were interpreted as providing support for the cognitive map theory, so that the internal cognitive map would be encoded by the hippocampus. Soon after, O'Keefe and Nadel published their seminal book *the Hippocampus as a Cognitive Map* (O'Keefe and Nadel, 1978), setting the groundwork for a broad research program on the neurobiological bases of spatial cognition. The firing activity of place cells may undergo a significant phenomenon called "remapping", consisting in significant changes in their firing activity (firing rate and/or place field location changes) that are well documented by now. It usually follows from geometrical and contextual changes

in the environment (Bostock et al., 1991; Muller and Kubie, 1987). For this reason, it is unlikely that they are the most elemental basis of path integration. Place cells are thought to encode information about location and environment at the population/ensemble level rather than individually (Wilson and McNaughton, 1993).

### **1.3.2 Head-direction cells**

The next spatially-tuned type of cell discovered was purported to represent a key type of information for spatial navigation: angular directionality, or at least, the heading direction of the animal. The cells encoding this information, called head-direction (HD) cells were first reported by Ranck (1984), and subsequently better characterized by Taube and his collaborators (Taube et al. 1990a, b). Although they were first found in the postsubiculum, further research located HD cells in the posterior cortex (Chen et al., 1994), the anterior nuclei of the thalamus (Taube, 1995), the entorhinal cortex (Sargolini et al., 2006) and the nucleus reuniens of the thalamus (Jankowski et al., 2014), among other areas. Each of these cells reach their peak firing rate when the animal faces the cell's preferred direction. HD cells typically have an approximately 90° wide response field, their preferred direction lying in the middle of the field, and their firing rate progressively decreasing as the animal's head direction deviates from the cell's preferred direction (Taube et al, 1990a).

Moreover, rotation of the environment or prominent visual cues translate to a similar rotation of the cells' firing field, which shows that HD cells are anchored to allothetic cues, that is, external stimuli (Taube et al., 1990b). However, HD cells also respond to idiothetic input like proprioceptive information when, for instance, allothetic input is not available (Yoder et al., 2011). Taken together, this suggests that HD cells may employ spatial representations to assist with path integration. The fact that HD cell activity correlates with path integration performance (Valerio et al., 2012) and the additional fact that path integration impairment follows from HD signal disruption provide further evidence in this direction (Butler et al., 2017).

### 13.3 Border cells

The existence of cells firing at the boundaries of the environment or at a certain distance from it have been reported in the subiculum (Barry et al., 2006), the MEC (Savelli et al., 2008; Solstad et al., 2008) and the pre- and parasubiculum (Boccaro et al., 2010). There is some terminological heterogeneity regarding the name of these cells: the terms “boundary vector cell”, “boundary cell” and “border cell” are used somewhat interchangeably, but I will not address this issue here.

Border cells are thought to correct error accumulation in grid cell activity (Hardcastle et al., 2015; Pollock et al., 2018). I shall come back to this in the section describing grid cells.

#### 1.3.4 Speed cells

Very recently, the existence of cells the activity of which is context-invariantly tuned to the running speed of the animal has been reported in the MEC (Kropff et al., 2015). These cells increase their firing rate linearly as a function of movement speed. Since they maintain their activity across contexts and in the dark, it has been proposed that they provide a speed code that is altogether independent of visual input. This kind of information, just like information on angular direction, is required for path integration. The fact that MEC speed cells and grid cells (but not hippocampal place cells) are linked by a common prospective bias suggests that the latter may integrate speed information in order to enable path integration.

### 1.3.5 Grid cells

Finally, we arrive to the most important type of cell for the purpose of this work: grid cells. First reported in 2005 in the medial entorhinal cortex (MEC), these cells display multiple place fields arranged hexagonally (Hafting et al., 2005). Their activity is preserved in the dark, and unlike that of place cells, is largely invariant across contexts (Hafting et al., 2005; Allen et al., 2014). For this reason, they have been called “low dimensional”, in contrast to place cells, which by virtue of encoding context-specific representations are “high dimensional” (Fyhn et al., 2007). Moreover, the periodicity of their activity fields suggests that grid cells must integrate information about the angular direction and speed of movement. It has been shown that the disruption of the head direction signal in turns impairs grid cell activity (Winter et al., 2015). All in all, by displaying a low-dimensional, context invariant signal, and likely integrating angular direction and speed information, it is likely that they are involved in path integration by providing a universal metric of the environment and the position of the animal therein (Fuhs and Touretzky, 2006; McNaughton et al., 2006; Burgess et al., 2007; Moser and Moser, 2008; Burak and Fiete, 2009). This hypothesis is supported by the fact that knockout mice lacking GluA1-containing AMPA receptors show both a selective disruption of grid cell activity – but not of the HD signal and speed modulation – and impaired path integration performance (Allen et al., 2014).

However, after prolonged absence of cues, the grid signal accumulates error due to intrinsic noise (Burgess et al., 2007; Burak and Fiete, 2009). Visual cues anchor both the grid cell signal and the head direction signal that it integrates, and correct error accumulation (Goodridge and Taube, 1995; Knierim et al., 1995; Skaggs et al., 1995; McNaughton et al., 1996; Hafting et al., 2005; Allen et al., 2014; Evans et al., 2016). Environmental boundaries correct grid cell signal error accumulation as well (Hardcastle et al., 2015), and may improve path integration performance. This may be the reason why grid cell activity persisted relatively undisrupted (showing a mild decrease in spatial selectivity) in darkness during relatively long periods of time in Hafting et al. (2005). and Allen et al. (2014). It is worth noting that the arena boundaries were walled in Hardcastle et al. (2015).

Nonetheless, non-metric cues and environmental borders may do more than just correcting error accumulation; it is not so clear to what extent grid cell activity is context-invariant. Non-standard arena shapes can distort grid symmetry, homogeneity, scale and field size (Krupic et al., 2015; Stensola et al., 2015). It has also been shown that the color and odor of the enclosure exert translational changes (but no orientation, scale or rate changes) in the grid signal. The former observation argues against the possibility of grid cells being the neurobiological substratum of the representation of a universal metric of space and perhaps of the path integration function, or at least for a more complicated picture on how grid cells work. The latter observation suggests that grid cells may represent more heterogeneous information than previously thought, although this evidence is still weak.

#### **1.4 Aim of this work**

The possibility that visual cues exert broader effects on the activity of grid cells than just anchoring it remains open. First, it may be that in darkness and in the absence of walls in the environmental boundaries and other contaminating variables, visual information is more critical than previously thought. If so, this would undermine the notion that grid cells are the main substratum for path integration. Second, it may be the case that the modification of non-metric, contextual visual cues exert changes in the grid cell code. If so, grid cells would encode heterogeneous information instead of an invariant, universal metric of space. This work sets out to test these two possibilities by recording the activity of grid cells and other spatially selective MEC neurons in mice running in environments where access to visual landmarks was manipulated.

## 2. MATERIALS AND METHODS

Two experiments employing two different mice cohorts were carried out (all data is available at the Dryad Digital Repository: 10.5061/dryad.c261c; Pérez-Escobar et al., 2016a): a circular arena experiment, and a linear track experiment. Sections 2.1-2.3 were common to both experiments. Sections 2.4-2.9 refer to the circular arena experiment, while sections 2.9 and 2.10 refer to the linear track experiment. Some methods for the detection of spatially selective cells in 2.5 were used for the cell detection phase the linear track experiment. Histological procedures (2.12) were common to both experiments.

### 2.1 Surgical procedure

This section is taken from Pérez-Escobar et al. (2016b) with minor changes and with kind permission from *eLife Sciences Publications*.

All experiments were carried out in 3–6 month-old male wild type C57BL/6 mice and were approved by the Governmental Supervisory Panel on Animal Experiments of Baden-Württemberg in Karlsruhe (35-9185.81/G 50/14). Mice were singly housed and kept on a 12 hr light-dark schedule with all procedures performed during the light phase. The mouse cages were 26 cm long, 20 cm wide and 14 cm high. The cage floor was covered with 2 cm of saw dust and 1–2 facial tissues were placed in the cage. Mice were implanted with 4 movable tetrodes in each hemisphere. The tetrodes were constructed from 4 12 mm-diameter tungsten wires (California Fine Wire Company, Grover Beach, California) and held in a microdrive assembly that allowed them to be moved individually. Before implantation, tetrodes were gold plated to reduce their impedance to 300–500 k $\Omega$ .

Mice were anesthetized with isoflurane (1–3%) and placed into a stereotaxic apparatus. The skull was exposed and four anchor screws were inserted into the skull. Two

screws located above the cerebellum served as ground and reference signals. The following coordinates were used (ML:  $\pm 3.1$  mm from bregma, AP: 0.2 mm from transverse sinus,  $6^\circ$  in the posterior direction). The tetrodes were lowered into the cortex and the microdrive was fixed to the skull with dental cement. Mice were given one to two weeks to recover after surgery.

## 2.2 Recording system, spike extraction and spike clustering

This section is taken from Pérez-Escobar et al. (2016b) with minor changes and with kind permission from *eLife Sciences Publications*.

The animals were connected to the data acquisition system (RHD2000-Series Amplifier Evaluation System, Intan Technologies, analog bandwidth 0.09–7603.77 Hz) via a lightweight cable and the signal was sampled at 20 kHz. Action potentials were detected off-line from the bandpass-filtered signal (800–5000 Hz). Waveform parameters were obtained from a principal component analysis and clusters of spikes were automatically generated using Klustakwik. Spike clusters were refined manually with a graphical interface program. Cluster separation quality was assessed from the spike-time autocorrelation and isolation distance. A refractory period ratio was calculated from the spike-time autocorrelation (from 0 to 25 ms, bin size: 0.5 ms). The mean number of spikes from 0 to 1.5 ms was divided by the maximum number of spikes in any bin between 5 and 25 ms. Clusters with a refractory period ratio larger than 0.125 were not kept. In addition, clusters with an isolation distance (Schmitzer-Torbert et al., 2005) shorter than 5 were excluded from the analysis.

Two infrared-LEDs (wave length 940 nm), one large and one small, were attached to the headstage. The large and small LEDs were located ahead and behind the head of the animal, respectively, with a distance of 8 cm between their centers. An infrared video camera (resolution of 10 pixels/cm, DMK 23FM021, The Imaging Source) monitored the LEDs at 50 Hz. The location and head direction of the animal were tracked on-line with custom software.

## 2.3 Initial training

This section is taken from Pérez-Escobar et al. (2016b) with minor changes and with kind permission from *eLife Sciences Publications*.

After the recovery period, mice were put on a food restriction diet to reduce their weight to 85% of their normal free-feeding weight. They were then trained 3 times a day (3 x 10 min) to run in a 70 x 70 cm open field to retrieve food rewards (AIN-76A Rodent tablets 5 mg, TestDiet) delivered at random locations from pellet dispensers located above the ceiling of the recording environment (CT-ENV-203-5 pellet dispenser, MedAssociates). The pellet dispensers were controlled by a microcontroller (Arduino Uno) and the inter-delivery intervals ranged from 20 to 40 s.

After 2 days of training, the procedure continued (3 x 15 min) but the mice were connected to the recording system. The tetrodes were lowered on each day and the raw signals were monitored on an oscilloscope. Recordings began when large theta oscillations were observed on most tetrodes (Fyhn et al., 2008). The tetrodes were also lowered by approximately 25–50  $\mu\text{m}$  at the end of each recording session.

## 2.4 Circular arena

This section is taken from Pérez-Escobar et al. (2016b) with minor changes and with kind permission from *eLife Sciences Publications*.

The apparatus consisted of an elevated (4.5 cm) gray circular PVC unwallied platform (80 cm diameter) located in the center of a gray square box (100 x 100 x 19.5 cm). The square box was filled with water up to 3 cm to prevent the animal from getting off the circular arena. The recording environment was surrounded by opaque black curtains. On every side of the box, a LED panel provided a polarizing cue to the animal (90° angle between the lights). The light panels consisted of black aluminum sheets (46 cm x 33 cm) with two horizontal LED strips (45 cm long, 25 cm apart from each other; color

temperature: 3000 K, Ribbon Slim Top, Ledxon Group, powered by 6 1.2 V batteries). These light panels were the only potential source of visible light in the recording environment. An audio speaker located directly above the arena emitted a white noise, overshadowing uncontrolled auditory cues.

After initial training, the mouse was transported from the holding room to the recording room in an opaque circular container (15 cm diameter) and underwent a disorientation procedure in which the container was spun 5 times clockwise and 5 times counterclockwise (approximately 1 rotation/s). The mouse was connected to the recording system outside of the curtains, and it was carried within the holding box into the enclosure and placed on the arena. After closing the curtains around the apparatus, the recording started and the experimenter left the room for the duration of the recording session. The mouse had no prior experience of the recording room before the first recording session.

The light panels were controlled by a microcontroller (Arduino Uno) via a 4-channel relay module. For each recording session, two of the four light panels were chosen randomly and only these two lights were used during the recording session (referred to as l1 and l2). The location of l1 and l2 varied randomly across days in the same animal. A session started with a baseline of 10 min with l1 turned on, followed by 2 min in darkness and a series of 60 2-min trials, alternating between light and dark trials. Only one light was switched on during a given light trial, and the order of presentation of the two lights was random. At the end of the light-dark trial sequence, an additional baseline of 10 min with l2 turned on was performed. The experimenter entered the recording room, the mouse was removed from the recording environment and the tetrodes were lowered by approximately 25–50  $\mu\text{m}$ . To ensure that mice visited every location on the elevated arena, food rewards were delivered at random positions during recording sessions.

## 2.5 Identification of spatially selective neurons

This section is taken from Pérez-Escobar et al. (2016b) with minor changes and with kind permission from *eLife Sciences Publications*.

Data analysis was performed in the R software environment and the source code is available at [https://github.com/kevin-allen/prog\\_perez\\_escobar\\_2016](https://github.com/kevin-allen/prog_perez_escobar_2016). Spatial firing rate maps were generated by dividing the environment into 2 x 2 cm bins. The time spent in each bin was calculated and the resulting occupancy map was smoothed with a Gaussian kernel (s.d = 3 cm). The number of spikes emitted as the animal was in each bin was divided by the corresponding bin of the occupancy map to obtain the firing rate map, which was then smoothed with a Gaussian kernel function (s.d = 3 cm). Only periods when the mouse ran faster than 3 cm/s were considered. The spatial information score (Skaggs et al., 1996) was defined as follows:

$$I = \sum_{i=1}^N p_i \frac{\lambda_i}{\lambda} \log_2 \frac{\lambda_i}{\lambda}$$

where  $p_i$  is the occupancy probability of bin  $i$  in the firing map,  $\lambda_i$  is the firing rate of bin  $i$ , and  $\lambda$  is the mean firing rate of the neuron.

Spatial autocorrelations were calculated from the firing rate maps. Peaks in the autocorrelation matrix were defined as > 10 adjacent bins with values > 0.1. The 60° periodicity in the spatial autocorrelation matrix was estimated as follows (Sargolini, 2006). A circular region of the spatial autocorrelation matrix containing up to six peaks and excluding the central peak was defined. Pearson correlation coefficients ( $r$ ) were calculated between this circular region of the matrix and a rotated version of itself (by 30°, 60°, 90°, 120°, and 150°). A grid score was obtained from the formula:

$$\left(\frac{r_{60^\circ} + r_{120^\circ}}{2}\right) - \left(\frac{r_{30^\circ} + r_{90^\circ} + r_{150^\circ}}{3}\right)$$

Significance thresholds for information and grid scores were obtained by shifting the position data by at least 20 s before recalculating both scores. This procedure was repeated 100 times for each neuron in order to obtain surrogate distributions. The 95th percentiles of the null distributions were used as significance thresholds. Neurons with a significant grid score during both 10-min baselines or during one baseline and 12 trials were defined as grid cells. The spacing of a grid cell was defined as the mean distance from the central peak to the vertices of the inner hexagon in the spatial autocorrelation.

Border cells were identified using a border score calculated from two variables ( $CM_{0.5}$  and DM). The pixels of a firing rate map that were directly adjacent to the periphery of the arena were identified. Firing fields, defined as groups of adjacent pixels with a firing rate larger than 20% of the peak firing rate of the map and covering at least 40 cm<sup>2</sup>, were detected. For each field, the proportion of the pixels along the periphery that were also part of the field was calculated. CM was defined as the maximum proportion obtained over all possible fields. Because the firing fields of a border cell in circular environment typically cover up to half of the periphery, the variable  $CM_{0.5}$  was defined as  $(1 - |(0.5 - CM)| * 2)$ .  $CM_{0.5}$  had a value of 1 when the firing field covered half of the periphery and a value of 0 when the field covered all of the periphery or nothing of the periphery. DM was the mean shortest distance to the periphery for pixels that were part of a firing field, weighted by the firing rate in each pixel. DM was then normalized as follows. For each pixel in the map, the shortest distance to the periphery was calculated. The largest value obtained over all map pixels was the value used for the normalization. The border score was defined as  $(CM_{0.5} - DM)/(CM_{0.5} + DM)$ . Significance level was obtained with the same shuffling procedure as for information and grid scores. Border cells were defined as cells with a significant border score during both baselines or during one baseline and 12 trials.

As most border cells in a circular environment cover only a section of the periphery (Solstad et al., 2008), a polarity score for each map was calculated too. For each pixel of the map, a vector was created. Its direction was that of the pixel relative to the center of the map and its length was set to the firing rate in that pixel. The map polarity score was defined as the length of the resulting vector after summing individual vectors and normalizing the length by the sum of the firing rate of all pixels in the map.

Irregular spatially selective cells were neurons that were not classified as grid or border cells and that had a significant spatial information score during both baselines or during one baseline and 12 trials.

Head-direction cells were identified by constructing a histogram with the firing rate of a neuron as a function of head direction ( $10^\circ$  per bin). The mean vector length of the histogram was used as a measure of head direction selectivity. A null distribution of mean vector length was obtained by shifting the head direction data by at least 20 s before recalculating the mean vector length. This shuffling procedure was repeated 100 times for each neuron and the 95th percentile of the surrogate distribution served as significance level. Head-direction cells had a significant vector length and a peak firing rate above 5 Hz during both baselines or during one baseline and 12 trials.

To identify speed-modulated cells, the instantaneous firing rate of the neurons was calculated. The number of spikes in 1 ms time windows was counted and a convolution between this spike count array and a Gaussian kernel (s.d = 100 ms) was performed. The resulting vector was integrated over 100 ms time windows. Periods during which the mice ran slower than 3 cm/s were removed from the analysis. Running speed was estimated every 20 ms. A speed score was defined as the Pearson correlation coefficient between the instantaneous firing rate and the running speed of the animal. Chance levels were obtained with a shuffling procedure ( $n = 100$ ) in which the speed vector was shifted by at least 20 s before calculating speed scores. To be considered a speed-modulated cell, the neuron had to have a speed score above the 95th percentile of the surrogate distribution during both baselines or during one baseline and 12 trials.

## 2.6 Stability of firing rate maps

This section is taken from Pérez-Escobar et al. (2016b) with minor changes and with kind permission from *eLife Sciences Publications*.

To assess the stability of the spatial firing patterns during dark trials, d1 trials were divided into 12 blocks of 10 s. Maps were constructed for the 12 blocks, concatenating homologous blocks across trials of a given condition. The stability of the map in each block was obtained by calculating the correlation coefficient between the block specific firing map and the map containing all 120-s l1 trials. As controls, the l1 trials were also divided into 12 blocks and the maps observed during each block were compared to the maps containing all 120-s l1 trials.

## 2.7 Spike distance metric

This section is taken from Pérez-Escobar et al. (2016b) with minor changes and with kind permission from *eLife Sciences Publications*.

Error accumulation in the spikes of grid cells was estimated by the spike distance metric (SDM) (Hardcastle et al., 2015). For each cell, a firing rate map was constructed using the first 60 s of l1 trials. A firing field was defined as an area of at least 20 cm<sup>2</sup> in which each bin had a firing rate above the 75th percentile of the rate distribution of all bins in the map. The center of mass of each firing field was calculated. The radius of a firing field was equal to the radius of a circle with an area equal to that of the firing field. For each spike, the distance of the animal location at the time of the spike to the closest firing field center of mass was calculated. SDM was this distance divided by the mean radius of all detected fields in the firing rate map. SDM was calculated for spikes fired in the last 60 s of l1 trials and the entire d1 trials.

## 2.8 Distance coding by grid cells

This section is taken from Pérez-Escobar et al. (2016b) with minor changes and with kind permission from *eLife Sciences Publications*.

Spike-triggered firing rate maps were constructed by taking each spike of a neuron as a reference spike and considering only data of the next 10 s. The position data within each time window were shifted so that the reference spike was aligned to position (0,0). The space surrounding the reference spikes was divided into 2 x 2 cm bins and both the occupancy maps and the resulting spike-triggered firing rate maps were smoothed with a Gaussian kernel (s.d = 2 cm). To obtain a distance tuning curve, the bins of the spike-triggered firing rate map were used to calculate the mean firing rate as a function of distance from the reference spikes. The distance was normalized by dividing it by the spacing of the grid cell measured during the first baseline of the recording session. A distance score was defined as  $(\lambda_1 - \lambda_{0.5}) / (\lambda_1 + \lambda_{0.5})$  where  $\lambda$  indicates the firing rate of a neuron at a given normalized distance. Chance levels for distance scores were obtained by shifting the spike trains by at least 20 s relative to the position data before recalculating the scores. Only grid cells with a spacing shorter than 50 cm were used in the distance analysis.

## 2.9 Detection of putative excitatory connections

This section is taken from Pérez-Escobar et al. (2016b) with minor changes and with kind permission from *eLife Sciences Publications*.

Putative excitatory connections were detected as narrow peaks in the spike-time crosscorrelations of simultaneously recorded neurons (from -50 to 50 ms, bin size = 0.5 ms) (Csicsvari et al., 1998; Marshall et al., 2002; Maurer et al., 2006; Mizuseki et al., 2009; Latuske et al., 2015). The crosscorrelations of all pairs of simultaneously recorded neurons were constructed. Crosscorrelations containing fewer than 300 spikes were excluded from the analysis. The bins from -10 to 0 ms and from 10 to 50 ms served to

calculate baseline mean and s.d. A peak at short latency in a crosscorrelation was defined as at least one bin between 0.5 and 4 ms that was above 6 s.d. from the baseline mean. A pair of cells was not considered if the baseline was not stable, i.e. if a bin between -10 and 0 ms or between 10 and 50 ms exceeded 75% of the short latency peak.

## 2.10 Linear track experiment

This section is taken from Pérez-Escobar et al. (2016b) with minor changes and with kind permission from *eLife Sciences Publications*.

A second cohort of mice was trained to run on a linear track. The linear track (80 x 5.4 cm) was made of wood and painted gray. The walls along the long axis of the maze were 1 cm high, except for the last 6.5 cm at the two extremities where the walls were 3 cm high. The walls of the short axis of the track were 16 cm high. A food well and an infrared beam were located 2 and 5 cm away from both ends of the track, respectively. Breaking the beam triggered the release of a food pellet at the opposite end of the track. Two gray walls (80 cm long x 28 cm high) were located 25 cm away from the long edges of the linear track. A single row of 48 LEDs (80 cm long) was attached to one of the side walls. On the opposite wall, 4 rows of 12 LEDs (20 cm long) were attached, aligned to one end of the track. The LEDs were the only potential source of visible light in the recording environment when the mouse ran on the linear track.

After initial training (see above), the mice were trained on the linear track 3 times a day for 10 min. During the first 2 days, food pellets were placed randomly on the track during training. The pellets were progressively moved away from the center of the maze over the next 2 days. Thereafter, pellets were only delivered upon infrared beam breaks. The recording cable was connected to the mouse during the subsequent training sessions (15 min) and training continued until the mouse performed approximately 40-55 runs within 15 min.

Recording sessions with the linear track started with 20 min of exploration in a 70 x 70 cm open field with normal light illumination, followed by 20 min in a rest box (25 x 25 cm). The recording session continued with 3 20-min trials on the linear track separated by 20-min trials in the rest box. There were 3 lighting conditions (l1, l2 and d) on the linear track. The order of presentation was random and the condition changed every 5th run on the track. In l1, a single row of LEDs was turned on. There was no other visible light source in the room. In l2, the 4 rows of LEDs were turned on instead of the single LED row. In d, all LEDs were turned off. Only recording sessions with at least 20 blocks of 5 runs on the track were considered for analysis.

Identification of spatially selective neurons in mice trained on the linear track was performed using the data from the square open field. The 95th percentiles of the surrogate distributions served as significance levels for each spatial score. The border score was defined as  $(CM - DM)/(CM + DM)$ .

## 2.11 Linear firing rate maps

This section is taken from Pérez-Escobar et al. (2016b) with minor changes and with kind permission from *eLife Sciences Publications*.

The position data on the linear track were linearized by calculating the regression line of the two-dimensional position data. Each position coordinate was moved to the closest point on the regression line. Linear firing rate maps were calculated like two-dimensional firing rate maps (same parameters and smoothing), with the exception that the data were unidimensional and runs toward each end of the track were treated separately.

## 2.12 Histology

This section is taken from Pérez-Escobar et al. (2016b) with minor changes and with kind permission from *eLife Sciences Publications*.

To confirm tetrode location, mice were deeply anesthetized with ketamine and xylazine, and perfused transcardially using saline, followed by 4% paraformaldehyde. The brains were removed and stored in 4% paraformaldehyde at 4°C overnight. The brains were then sliced in 50  $\mu$ m-thick slices and stained with cresyl violet.

## 3. RESULTS

### 3.1 Circular arena experiment: broad effects of lack of visual information on spatially selective MEC neurons

This section is taken from Pérez-Escobar et al. (2016b) with minor changes and with kind permission from *eLife Sciences Publications*.

First, recordings from the MEC were performed in mice exploring an elevated circular arena (Figure 1A). The only potential sources of visible light were 4 identical LED panels located around the arena. Recording sessions included a sequence of 60 2-min trials, alternating between light and dark trials (Figure 1B). On most recording sessions, 2 different light panels were used (l1 and l2) with a 90° or 180° angle between them. Dark trials following l1 and l2 trials were referred to as d1 and d2 trials, respectively. Histological examination showed that most recording sites were in the MEC (75.51%, 37 out of 49) or at the transition between the MEC and the parasubiculum (12.24%, 6 out of 49) (see Figure 1C for some samples; the complete source data can be accessed from "<https://elifesciences.org/articles/16937/figures>" under "Figure 1 – source data 1" and "Figure 1 – source data 2"). Another 12.24% (6

out of 49) of the recording sites were in the parasubiculum. Of the tetrode tracks in the MEC, 86.49% had reached layer II by the last recording session. A total of 880 neurons were recorded in 8 mice (89 recording sessions).

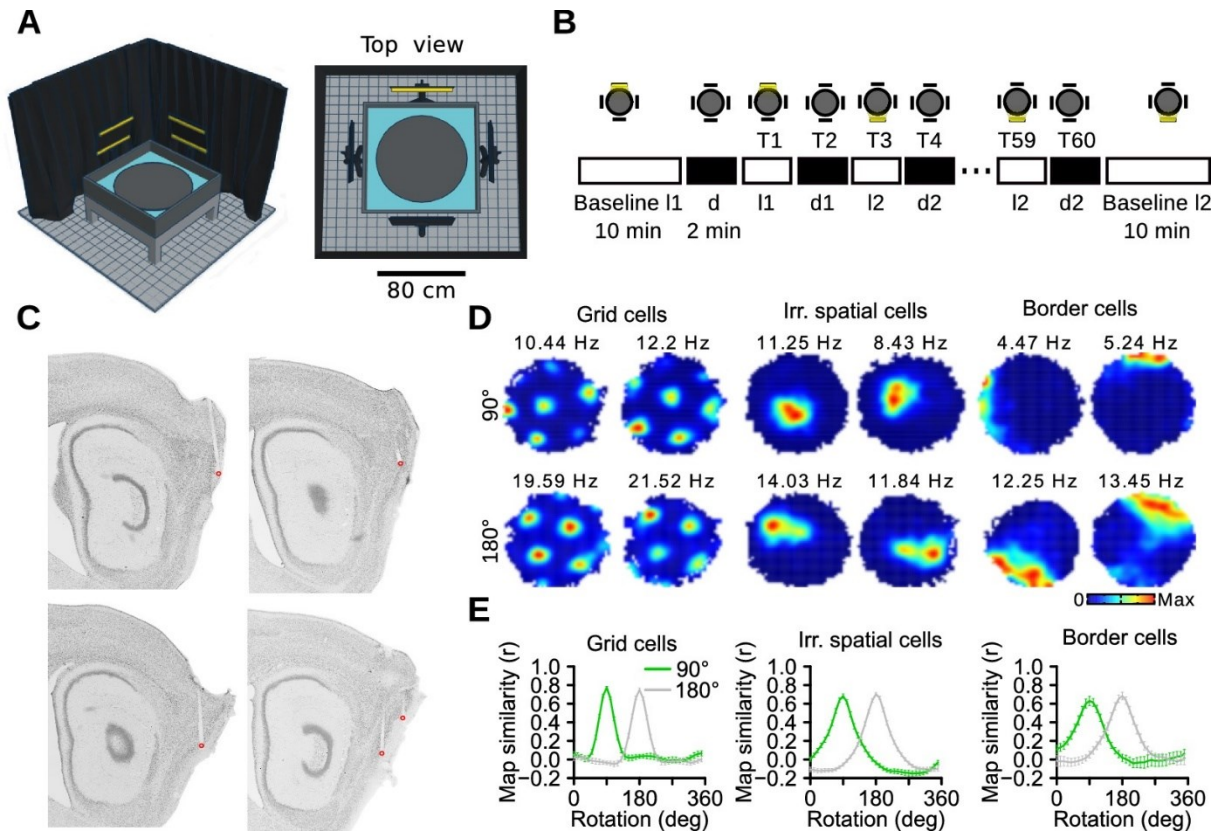


**Figure 1. Recording protocol and cue control of MEC spatial representations.** (A) Schematic of the recording apparatus. Left: Side perspective. An elevated circular arena was located within a square box filled with water. Note that half of the black curtain and two light panels were omitted for better visualization. Right: Top view. Four LED panels were positioned outside the box at 90° to each other. (B) Recording protocol. Two lights out of four were selected at the beginning of each recording session (I1 and I2). The protocol started and ended with a 10-min baseline, one with each light (Baseline I1 and Baseline I2). In between were 60 2-min trials (T), alternating between light and dark trials. The presentation of the two lights (I1 and I2) followed a random sequence. Only one light could be switched on at any time. (C) Sagittal brain sections showing the location of the recording sites (red dots) in the MEC. (D) Examples of firing rate maps of two grid cells (left, one cell on each row), two irregular spatially selective neurons (middle) and two border cells (right) during trials with I1 and I2. Top and bottom rows contained cells recorded with I1 and I2 being at 90° and 180° to each other, respectively. The numbers above the firing rate maps are the peak firing rates. (E) Correlations between I1 and I2 maps after rotating I2 maps in 10° steps, plotted separately for sessions with 90° and 180° between I1 and I2. Taken from Pérez-Escobar et al., (2016b) with kind permission from *eLife Sciences Publications*

### 3.1.1 Visual landmarks anchor MEC spatial representations

This section is taken from Pérez-Escobar et al. (2016b) with minor changes and with kind permission from *eLife Sciences Publications*.

It was first tested whether the orientation of MEC spatial representations was controlled by the position of the light source (Muller and Kubie, 1987; Goodridge and Taube, 1995; Hafting et al., 2005). It was found that the firing fields of grid cells, border cells and irregular spatially selective neurons rotated around the center of the arena to follow the position of the light (Figure 1D). Correlations between maps of l1 and l2 trials were calculated after rotating l2 maps (Figure 1E). Peak correlations were obtained near 90° and 180° for recording sessions in which the angle between l1 and l2 was 90° and 180°, respectively. Thus, during light trials, the light panels acted as dominant polarization cues.

### 3.1.2 Rapid degradation of grid cell periodicity in absence of visual Landmarks

This section is taken from Pérez-Escobar et al. (2016b) with minor changes and with kind permission from *eLife Sciences Publications*.

It was investigated whether grid cells maintained a stable grid firing pattern in darkness. Surprisingly, the periodic firing was not visible in most rate maps of dark trials (Figure 2A). Grid scores and information scores were much lower during d1 trials compared to l1 trials (Figure 2B; paired Wilcoxon signed rank test, l1 vs d1,  $n = 139$  grid cells, grid score:  $v = 9223$ ,  $p < 10^{-16}$ , information score:  $v = 9722$ ,  $p < 10^{-16}$ ). The reductions in grid periodicity and spatial information content were also significant when comparing the medians of individual mice in which at least 5 grid cells were recorded (Figure 2C; paired Wilcoxon signed rank test,  $n = 6$  mice, grid score:  $v = 21$ ,  $p = 0.031$ , information score:  $v = 21$ ,  $p = 0.031$ ). Moreover, these alterations remained significant when limiting the analysis to neurons recorded from hemispheres in which

all tetrode tips were located in the MEC (referred to as MEC tetrodes) (paired Wilcoxon signed rank test,  $n = 75$  grid cells, grid score:  $v = 2708$ ,  $p < 10^{-11}$ , information score:  $v = 2846$ ,  $p < 10^{-14}$ ). Thus, visual landmarks were required to stabilize the grid firing pattern.

The grid pattern observed during light trials was present during the first few seconds in darkness. Trials were divided into 12 10-s blocks. The block firing maps were correlated to the complete l1 maps to obtain a measure of map similarity relative to l1 trials (Figure 2D). During d1 trials, map similarity was initially high and decreased during the first 30 s (paired Wilcoxon signed rank test,  $n = 132$ , b1-b2:  $p < 10^{-16}$ , b2-b3:  $p = 0.00053$ ). Block 3 was not different from block 4 ( $p = 0.17$ ). This indicates that the stable periodic pattern was only present during the first 30 s in darkness. Similar conclusions were reached when using the spike distance metric (Hardcastle et al., 2015) to quantify the accumulation of error in grid cell spikes during d1 trials (Figure 3). Interestingly, when the l1 LED panel was turned back on, map similarity during the first 10 s was lower than during the subsequent l1 block (Figure 2D,  $p < 10^{-15}$ ). Thus, the reinstatement of the grid pattern by visual stimuli occurred over the course of several seconds.

Pairs of grid cells with a similar spacing exhibit very stable firing associations; cells that fire together in one environment also fire together in a different environment (Fyhn et al., 2007; Yoon et al., 2013; Allen et al., 2014). Therefore, it was assessed whether the firing associations between grid cells were maintained even when the grid patterns were not stable. The instantaneous firing rate of grid cells was calculated (time window: 100 ms, gaussian smoothing kernel s.d: 100 ms) and the correlation coefficients between instantaneous firing rate vectors served as a measure of firing rate association. As expected, firing rate associations for pairs of grid cells were stable from l1 to l2 trials (Figure 2E, Pearson correlation of firing rate associations in l1 and l2 trials,  $n = 186$  grid cell pairs,  $r = 0.968$ ,  $p < 10^{-16}$ ). Despite instability in the spatial firing patterns of grid cells during dark trials, the firing rate associations of grid cells were to a large extent preserved during d1 trials (Figure 2E,  $r = 0.926$ ,  $p < 10^{-16}$ ). The median firing rate

of grid cells was slightly lower during dark trials than during light trials (Figure 2F; paired Wilcoxon signed rank test  $v = 6048$ ,  $p=0.0129$ ).

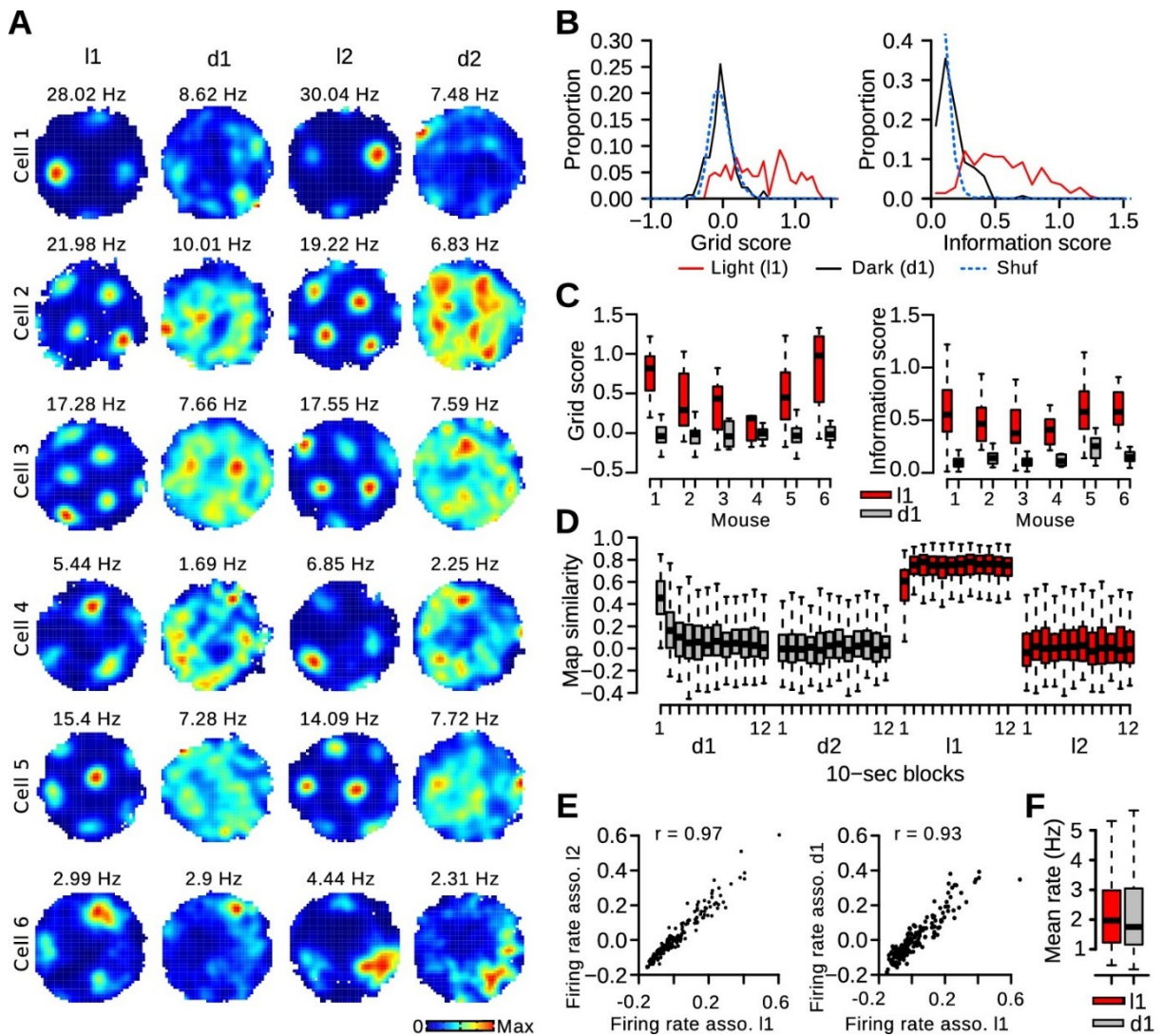


**Figure 2. Rapid degradation of grid cell periodicity in absence of visual landmarks.** (A) Firing maps of 6 grid cells during light and dark trials. (B) Distribution of grid and information scores of grid cells during l1 and d1 trials. The dotted blue line represents the surrogate (Shuf) distribution. (C) Grid and information scores during l1 and d1 trials for individual mice with at least 5 recorded grid cells. (D) Map similarity between 10-s block maps and l1 maps (left column in panel A). (E) Left: Firing rate associations of pairs of grid cells during l1 and l2 trials. Right: Firing rate associations of pairs of grid cells during l1 and d1 trials. (F) Mean firing rate of grid cells. Taken from Pérez-Escobar et al., (2016b) with kind permission from *eLife Sciences Publications*

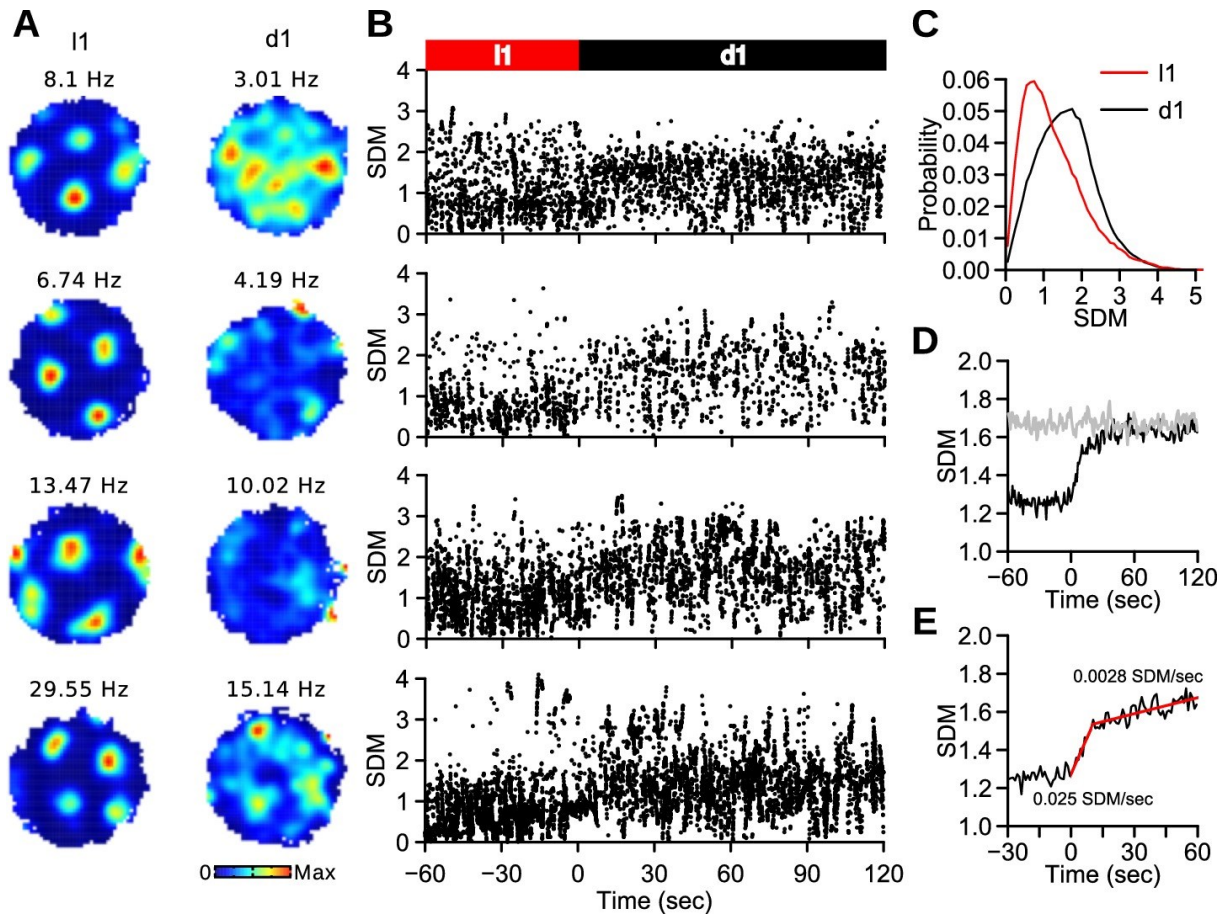


**Figure 3. Spike distance metric (SDM) during light and dark trials reveals rapid grid pattern disruption in darkness.** (A) Firing maps of 4 grid cells during light and dark trials. (B) SDM values of individual spikes as a function of time; darkness onset at time 0. (C) SDM value probability during light and dark trials. (D) SDM value over time for real (black) and surrogate (grey) data; darkness onset at time 0. (E) SDM value increases as a function of time; note how most of the increase happens in the first few seconds; darkness onset at time 0. Taken from Pérez-Escobar et al., (2016b) with kind permission from *eLife Sciences Publications*

### 3.1.3 Partly preserved distance coding by grid cells in darkness

This section is taken from Pérez-Escobar et al. (2016b) with minor changes and with kind permission from *eLife Sciences Publications*.

The loss of grid periodicity in darkness could be due to a slow translational drift of the grid pattern relative to the recording environment. If this is the case, the grid pattern should be visible in spike-triggered rate maps in which the effect of slow translational drift is minimized by resetting the position data each time a cell fires a spike (Figure

4A) (Bonnevie et al., 2013; Allen et al., 2014). In these maps, each spike in turn served as a reference spike and the position of the animal in the 10 s following a reference spike was shifted so that the position of the animal at the time of the reference spike was (0,0). Spike-triggered maps of grid cells during light trials often showed a central field surrounded by 6 fields (Figure 4A). During dark trials, the surrounding fields were less distinct or sometimes appeared as a ring of elevated activity. Accordingly, grid scores calculated from the spike-triggered maps were lower during d1 than l1 trials (n = 139 grid cells, median l1: 0.054, median d1: -0.062,  $v = 12246$ ,  $p=0.00011$ ). Thus, the impairment in grid periodicity in darkness cannot be fully explained by a slow translational drift.

It was next tested whether the modulation of firing rate as a function of distance was preserved in darkness. Distance coding by grid cells was visualized by plotting distance tuning curves, i.e. the mean firing rate of a grid cell as a function of the distance from reference spikes (Figure 4A). To perform population analysis, distance was normalized to the grid spacing measured during the first baseline. The increase in firing rate at the first period of the grid cells (Figure 4B; normalized distance = 1) was quantified with a distance score, which was defined as  $(\lambda_1 - \lambda_{0.5})/(\lambda_1 + \lambda_{0.5})$ , where  $\lambda_{0.5}$  and  $\lambda_1$  represent the firing rate of a neuron at normalized distance 0.5 and 1, respectively. Distance scores were smaller during dark trials than during light trials (Figure 4C; paired Wilcoxon signed rank test, n = 50 grid cells,  $v = 1181$ ,  $p<10^{-7}$ ), but distance scores in darkness were still above chance levels ( $v = 1006$ ,  $p=0.00038$ ). Taken together, the results indicate that estimation of distance by grid cells over short periods (10 s) was partially preserved in darkness. Moreover, the ring of activity in the spike-triggered maps of some grid cells in darkness suggests that the orientation of the grid pattern was not stable.



scores (Pearson correlation,  $n = 880$ ,  $r = -0.146$ ,  $p < 10^{-5}$ ), but several spatially selective neurons had significant speed scores (grid cells: 67 out of 139, irregular spatially selective cells: 54 out of 226, border cells: 11 out of 63, head-direction cells: 30 out of 85). Speed scores were positively correlated with mean firing rates ( $n = 880$ ,  $r = 0.238$ ,  $p < 10^{-13}$ ).

The presence of visual cues changed the speed code (Figure 5A). Most speed-modulated cells had a lower firing rate at a given speed during dark trials (Figure 5C, at 20–25 cm/s, 222 out of 304 cells, contingency chi-square test,  $\chi^2 = 64.47$ ,  $df = 1$ ,  $p < 10^{-16}$ ). The slopes of the regression line between speed and firing rate were steeper during light than dark trials (Figure 5D; paired Wilcoxon signed rank test,  $n = 304$ , median, light: 0.065, dark: 0.038,  $v = 35346$ ,  $p < 10^{-15}$ ). The intercepts (predicted firing rate during immobility) were also higher during light than dark trials (Figure 5E; median, light: 2.621, dark: 2.428,  $v = 31050$ ,  $p < 10^{-7}$ ). Speed scores were higher during light than dark trials (Figure 5F; median, light: 0.086, dark: 0.060,  $v = 32735$ ,  $p < 10^{-10}$ ). These changes in slopes, intercepts and speed scores were also present when considering only neurons recorded from MEC tetrodes ( $n = 144$  speed-modulated cells, slope:  $p < 10^{-13}$ , intercept:  $p = 0.0017$ , speed score:  $p < 10^{-9}$ ) or when using the median score of each mouse as a statistical unit ( $n = 8$  mice, slope:  $p = 0.0078$ , intercept:  $p = 0.016$ , speed score:  $p = 0.039$ ). The rate modulation by visual stimuli was sufficiently large that speed-modulated cells had a lower mean firing rate during dark trials (paired Wilcoxon signed rank test,  $n = 304$ , median, light: 3.47 Hz, dark: 2.89 Hz,  $v = 33797$ ,  $p < 10^{-12}$ ) even though running speed was higher during these trials (paired Wilcoxon signed rank test,  $n = 89$  recording sessions, median, light: 12.70 cm/s, dark: 14.81 cm/s,  $v = 124$ ,  $p < 10^{-14}$ ). The median change of firing rate from d1 to l1 trials, expressed as a percentage, was 12.36%. Thus, the rate response of speed-modulated neurons is determined by both internal self-motion cues and visual information.

Several speed-modulated cells have a high firing rate, which suggests that these might be PV-expressing MEC interneurons (Buetfering et al., 2014; Kropff et al., 2015). Whether PV-expressing interneurons were more likely to be classified as speed cells

than other MEC neurons was put to the test by re-examining the data from Buetfering and co-workers (Buetfering et al., 2014). The activity of 140 optogenetically-identified PV-expressing interneurons was examined alongside that of 996 other MEC neurons (Figure 5G). The speed score was used to identify speed-modulated cells (380 out of 1136 neurons, threshold = 0.079) in mice exploring an open field. The proportion of speed modulated cells was higher in the PV population than in other non-identified MEC neurons (Figure 5H; PV-expressing: 72 speed cells out of 140 neurons, 51.4%, other neurons: 308 out of 996 neurons, 27.1%, contingency chi-square test,  $\chi^2 = 22.27$ ,  $df = 1$ ,  $p < 10^{-6}$ ).

PV-expressing MEC neurons receive strong excitatory inputs from local neurons (Couey et al., 2013; Pastoll et al., 2013; Buetfering et al., 2014). Therefore, it was investigated whether the reduction in the firing rate of some high firing rate speed-modulated cells in darkness could be explained by changes in local excitatory inputs. Putative monosynaptic excitatory connections between MEC neurons were identified from spike-train crosscorrelations (Figure 5I) (Royer et al., 2012; Buetfering et al., 2014). Out of 10,880 crosscorrelograms, 61 (0.56%) showed a low latency peak indicative of excitatory connections. All connected pairs were made up of neurons recorded on the same tetrode. The percentage of putative excitatory connections for pairs of cells recorded on the same tetrode was 1.85 %.

Within functionally coupled neurons, speed-modulated cells were more likely to be post-synaptic (24 out of 42) than pre-synaptic (18 out of 58 neurons) neurons ( $\chi^2 = 5.7868$ ,  $df = 1$ ,  $p = 0.0162$ ). The firing rate of the cells presynaptic to speed-modulated cells was lower during dark than light trials (Figure 5J; paired Wilcoxon signed rank test,  $n = 37$ ,  $v = 555$ ,  $p = 0.0016$ ). The firing rate of the post-synaptic speed-modulated cells was also lower during dark trials (Figure 5K;  $n = 24$ , median, light: 18.44 Hz, dark: 15.44 Hz,  $v = 264$ ,  $p = 0.00057$ ). Moreover, the firing rate of presynaptic neurons increased with running speed (Figure 5L; paired Wilcoxon signed rank test, difference rate 2.5 cm/s vs 27.5 cm/s,  $n = 37$  light:  $v = 113$ ,  $p = 0.00016$ , dark:  $v = 109$ ,  $p = 0.00012$ ). Thus, the change in firing rate of some speed-modulated interneurons in darkness can be explained by a reduced local excitatory input.

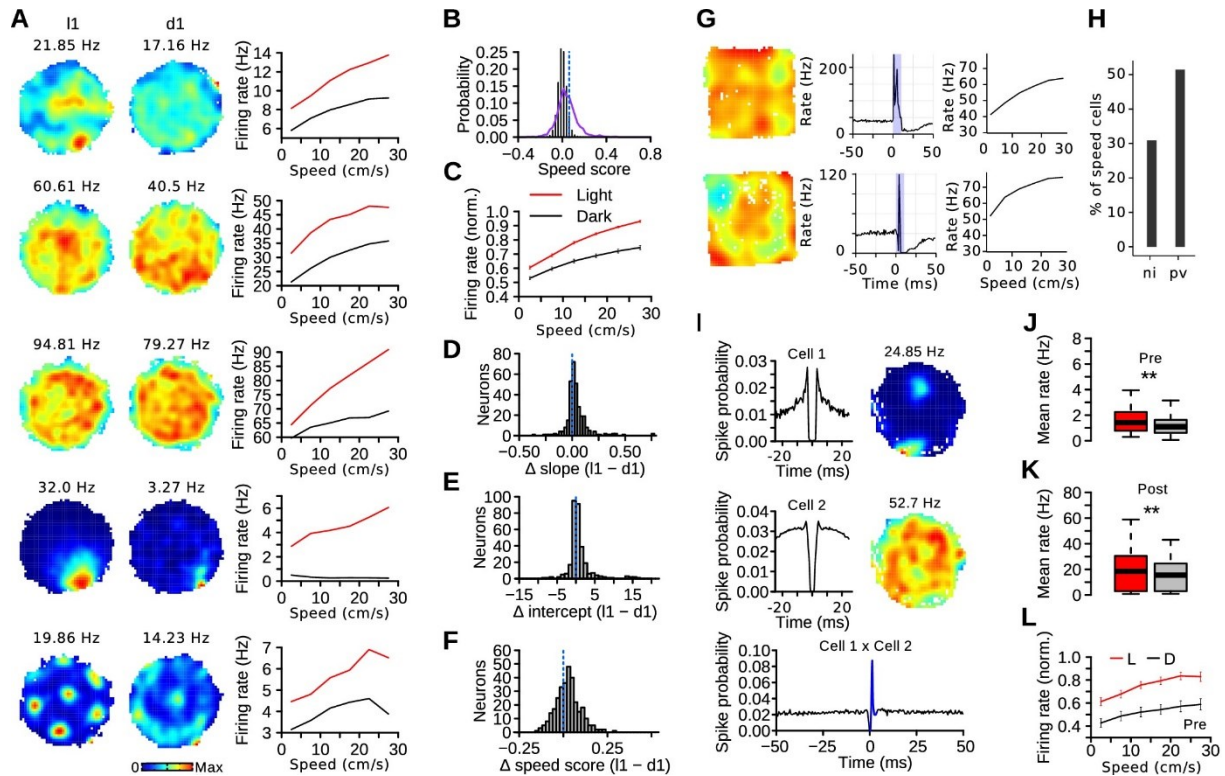


**Figure 5. Visual stimuli alter the MEC speed code.** (A) Examples of firing rate maps and speed tuning curves during light and dark trials for cells with a significant speed score. (B) Real (purple line) and surrogate (solid black bars) distributions of speed scores from MEC neurons. The dotted blue line indicates the threshold for statistical significance. (C) Mean normalized firing rate ( $\pm$  s.e.m) of speed-modulated cells as a function of running speed during l1 and d1 trials. (D, E and F) Difference of speed rate slopes, intercepts and speed scores of speed-modulated cells during l1 and d1 trials. The dotted lines indicate chance levels. (G) Firing rate map, response to laser stimulation and speed tuning curve of two PV-expressing neurons. (H) Percentage of speed-modulated cells in PV-expressing neurons (pv) and in non-identified MEC neurons (ni). (I) Example of a putative excitatory connection involving a post-synaptic speed cell. Left: spike-time autocorrelations of putative pre- (top) and post-synaptic (middle) neurons. Right: firing rate maps during light trials. Bottom: spike-time crosscorrelation of the two neurons. The blue color indicates the peak detection period. (J) Mean firing rate during light and dark trials of putative presynaptic neurons with excitatory interactions with a speed cell. (K) Mean firing rate during light and dark trials of speed cells receiving putative excitatory connections from a local neuron. (L) Mean firing rate ( $\pm$  s.e.m) as function of running speed of putative presynaptic neurons with excitatory interactions with a speed cell. \*\* $p < 0.01$ . Taken from Pérez-Escobar et al., (2016b) with kind permission from *eLife Sciences Publications*

### 3.1.5 Impaired border representation in darkness

This section is taken from Pérez-Escobar et al. (2016b) with minor changes and with kind permission from *eLife Sciences Publications*.

As mentioned before, border cells are thought to anchor grid cell fields to the geometry of an environment (Barry et al., 2007; Solstad et al., 2008; Lever et al., 2009; Evans et al., 2016; Hardcastle et al., 2015). The effect of visual landmarks on the firing of border cells was assessed. The activity of border cells during light trials was restricted to the periphery of the circular arena and usually covered less than half of the total circumference. In darkness, the activity of several border cells was no longer limited to the periphery of the arena (Figure 6A). A quantification of how restricted the firing of border cells was to the periphery of the arena was performed (DM, see Materials and Methods section 2.4). The firing of border cells was less concentrated at the periphery during d1 trials (Figure 6B; paired Wilcoxon signed rank test,  $n = 63$  border cells,  $v = 271$ ,  $p < 10^{-7}$ ). In addition, the polarity of the firing maps was reduced during d1 trials compared to l1 trials (see Materials and Methods, Figure 6C;  $v = 1698$ ,  $p < 10^{-6}$ ). Similar findings were observed when limiting the analysis to border cells recorded from MEC tetrodes ( $n = 38$  border cells, DM:  $v = 156$ ,  $p = 0.0014$ , map polarity:  $v = 552$ ,  $p = 0.008$ ). When using the median of each mouse as a statistical unit, a significant reduction of DM in darkness was observed ( $n = 7$  mice,  $v = 1$ ,  $p = 0.031$ ), but the reduction in map polarity in darkness did not reach significance level ( $n = 7$  mice,  $v = 24$ ,  $p = 0.11$ ).

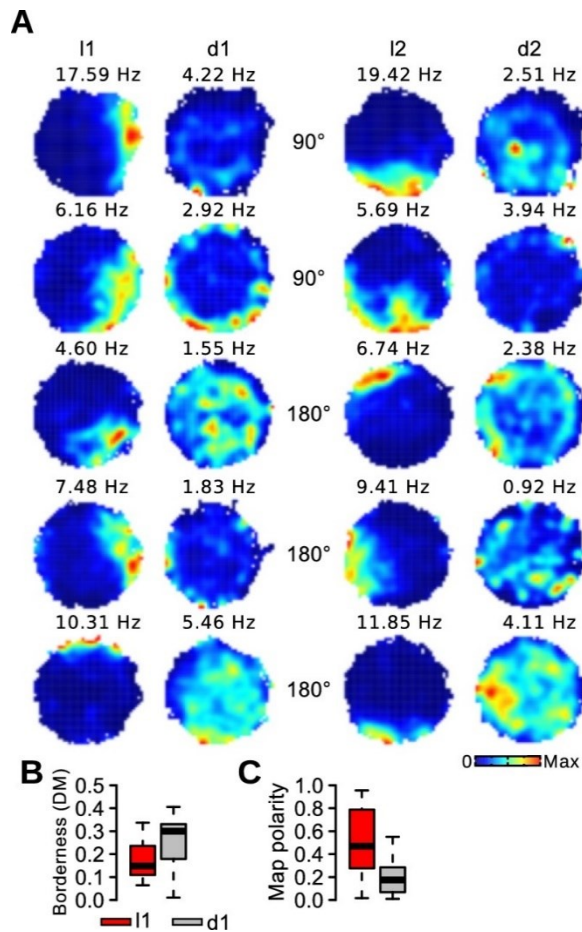


**Figure 6. Impairment of border representation in darkness.** (A) Firing maps of 5 border cells during light and dark trials. (B) Borderness (DM) of the firing rate maps of border cells during light and dark trials. (C) Polarity of the firing rate maps of border cells during light and dark trials. Taken from Pérez-Escobar et al., (2016b) with kind permission from *eLife Sciences Publications*

### 3.1.6 Reduced head-direction selectivity in darkness

This section is taken from Pérez-Escobar et al. (2016b) with minor changes and with kind permission from *eLife Sciences Publications*.

A total of 85 head-direction cells were recorded on the circular arena. Changes in head direction selectivity were quantified using the mean vector length of the rate/head direction histograms of head-direction cells. As shown in Figure 7A, most head-direction cells had reduced head direction selectivity during dark trials compared to light trials. Head direction vector length of head-direction cells were lower during d1 trials than l1 trials (Figure 7B, paired Wilcoxon signed rank test,  $v = 3617$ ,  $p < 10^{-15}$ ). A

similar conclusion was reached when limiting the analysis to MEC tetrodes ( $n = 54$  head-direction cells,  $v = 1457$ ,  $p < 10^{-10}$ ) or when using the median of each mouse as a statistical unit ( $n = 8$  mice,  $v = 36$ ,  $p = 0.0078$ ).

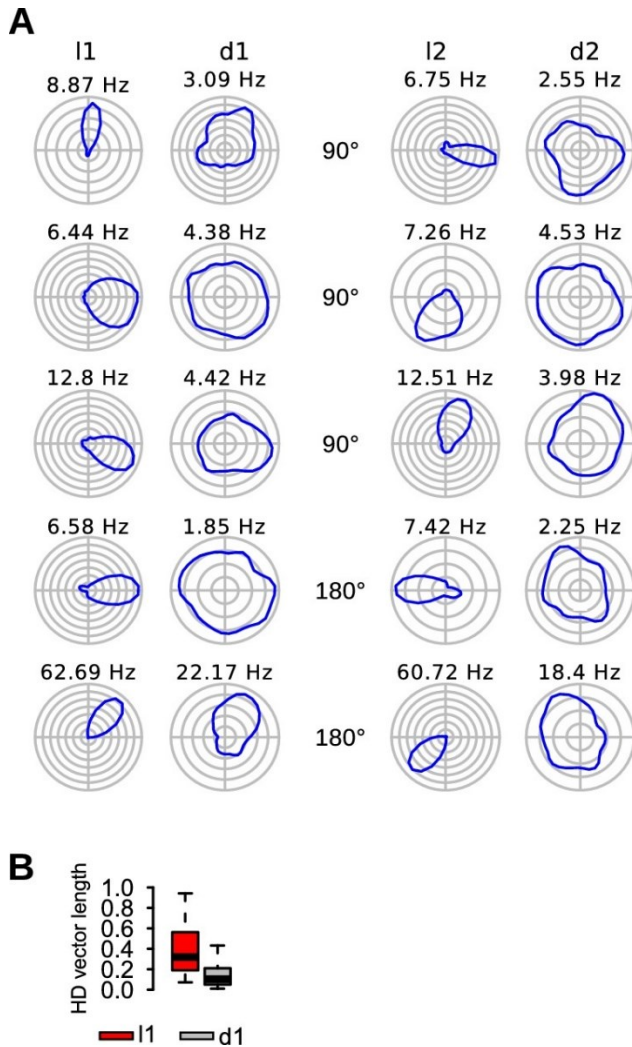


**Figure 7. Reduced head direction selectivity in darkness.** (A) Firing maps of 5 head-direction cells during light and dark trials. (B) Head direction vector length of head-direction cells during l1 and d1 trials. Taken from Pérez-Escobar et al., (2016b) with kind permission from *eLife Sciences Publications*

### 3.1.7 Firing rate changes in MEC neurons between light and dark trials

This section is taken from Pérez-Escobar et al. (2016b) with minor changes and with kind permission from *eLife Sciences Publications*.

Next, it was investigated whether the firing rate of MEC neurons changed significantly when visual landmarks were eliminated. For each neuron, a rate discrimination index was obtained using:  $(\lambda_{light} - \lambda_{dark}) / (\lambda_{light} + \lambda_{dark})$ , where  $\lambda_{light}$  and  $\lambda_{dark}$  are the mean firing rate during light and dark trials, respectively. Significance levels were obtained on a cell-by-cell basis by shuffling trial identities 500 times to obtain a distribution of discrimination indices. The 99th percentiles of the surrogate distributions served as significance levels. Only periods during which the running speed of the mice was between 5 and 20 cm/s were used. Examples of neurons with a significant rate change between light and dark trials are shown in Figure 8A. For some neurons, the firing rate changes between trial types were readily visible in their instantaneous firing rate (Figure 8B). When all recorded neurons were considered, the median rate discrimination index (0.072) was significantly larger than 0, demonstrating that MEC neurons tend to have higher firing rates when visual landmarks are present (Figure 8C, paired Wilcoxon signed rank test,  $n = 880$ ,  $v = 289120$ ,  $p < 10^{-16}$ ). This rate change was also significant when only neurons recorded from MEC tetrodes were considered ( $n = 447$ ,  $v = 76177$ ,  $p < 10^{-16}$ ) or when the median rate discrimination index of each mouse was used as a statistical unit ( $n = 8$  mice,  $v = 36$ ,  $p = 0.0078$ ). Out of 880 MEC neurons, 503 (57.2%) significantly changed their firing rate between light and dark trials. These neurons were more likely to reduce (76.74%) than increase (23.26%) their firing rate in darkness ( $\chi^2 = 143.86$ ,  $df = 1$ ,  $p < 10^{-16}$ ). The proportion of significant neurons in the different functional cell types is shown in Figure 8D. Border cells were more likely than grid cells to change their firing rate depending on the presence of visual landmarks ( $\chi^2 = 11.845$ ,  $df = 5$ ,  $p = 0.037$ ).

It was also tested whether putative interneurons (cells with a mean firing rate  $> 10$  Hz,  $n = 133$ ) and putative principal cells (cells with a mean firing rate  $< 5$  Hz,  $n = 694$ ) were equally likely to change their mean firing rate depending on the presence of visual landmarks. The probability of observing significant rate change between light and dark trials was similar for interneurons and principal cells (interneurons: 0.617, principal cells: 0.549,  $\chi^2 = 1.802$ ,  $df = 1$ ,  $p = 0.18$ ).

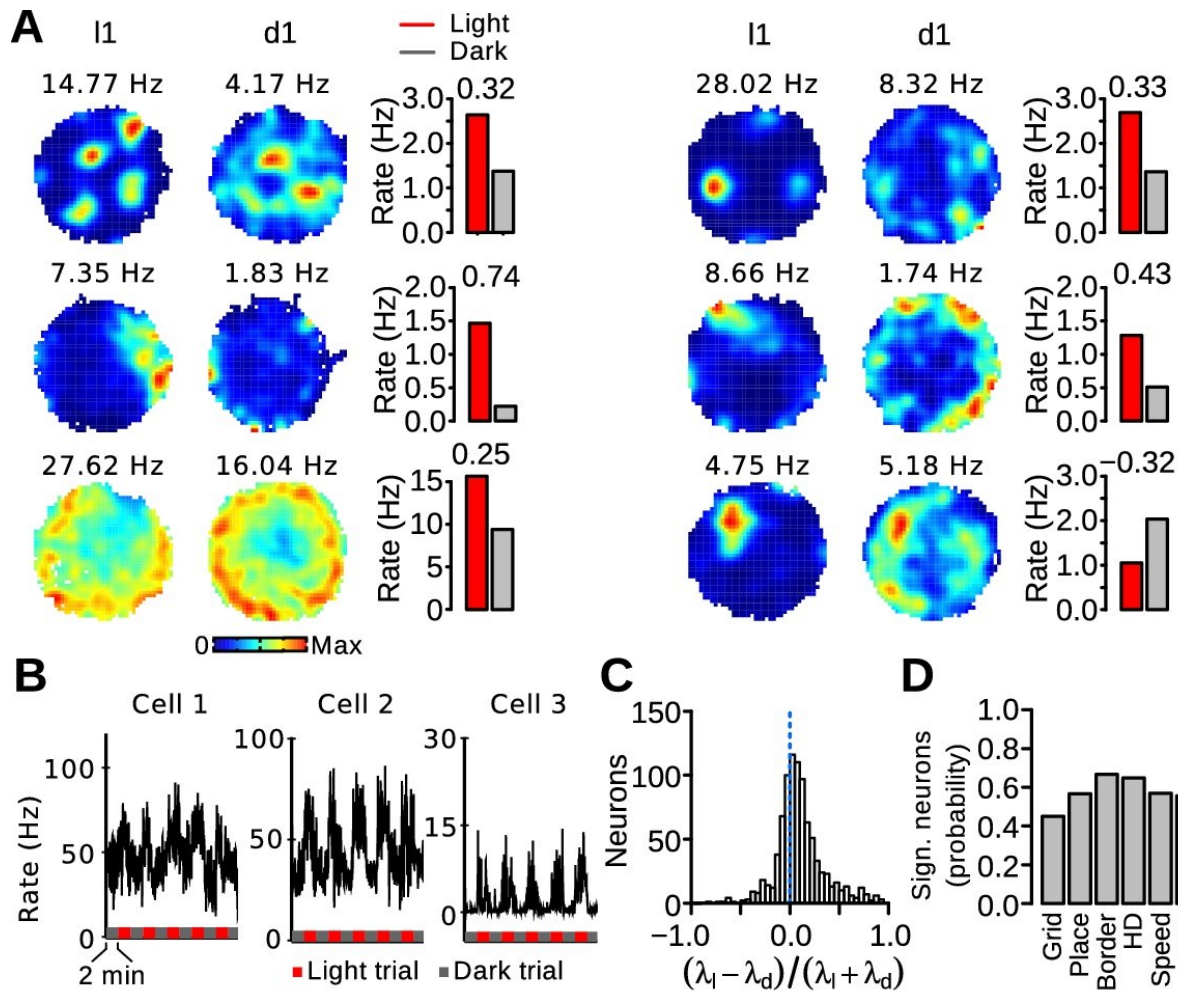


**Figure 8. Firing rate changes of MEC neurons between light and dark trials.** (A) Firing maps and mean firing rates during light and dark trials for 6 neurons. The number above each bar plot is the rate discrimination index. (B) Examples of instantaneous firing rates of 3 neurons during light and dark trials (smoothing kernel width s.d = 900 ms). (C) Distribution of the rate discrimination indices for all recorded neurons (including putative interneurons). Most neurons had a positive discrimination index, indicating higher firing rates during light trials. The dotted line indicates chance level. (D) Proportion of neurons with a significant rate change between light and dark trials in different functionally defined cell types (Grid: grid cells, Place: irregular spatially selective cells, Border: border cells, HD: head-direction cells, Speed: speed-modulated cells, UID: unidentified cells). Taken from Pérez-Escobar et al., (2016b) with kind permission from *eLife Sciences Publications*

### **3.2 Linear track experiment: Firing rate changes associated with nonmetric contextual cue manipulation in 1D environment**

This section is taken from Pérez-Escobar et al. (2016b) with minor changes and with kind permission from *eLife Sciences Publications*.

The results presented so far indicate that the firing rate of MEC neurons is modulated by the presence of visual landmarks. This suggests that the firing rate of spatially selective neurons in the MEC could also convey information about the distinct visual stimuli present in an environment. For this reason, a second experiment with a new cohort of mice was carried out in order to test whether the rate code of MEC neurons discriminates different nonmetric visual landmarks (or contexts) in an otherwise unchanged environment. The activity of 479 neurons (5 mice, 48 recording sessions) was recorded as mice ran back and forth on a linear track flanked by two side walls (Figure 9A). Histological analysis indicated that 14 recording sites were in the MEC, 4 in the MEC/parasubiculum border, and 13 in the parasubiculum (source data can be accessed from "<https://elifesciences.org/articles/16937/figures>" under "Figure 8 – source data 1" and "Figure 8 – source data 2"). There were 3 lighting conditions (l1, l2 and d). In l1, a single row of 48 LEDs on one wall was turned on. In l2, 4 rows of 12 LEDs located on the opposite wall were turned on. In d, all LEDs were turned off. The condition was changed randomly every 5th run. Thus, the only difference between l1 and l2 conditions was the LED pattern that was turned on and the geometry of the apparatus remained unchanged.

A 20-min exploration trial in a square open field preceded the linear track trials and served to identify the different functional cell types (Figure 9B). 138 grid cells, 28 border cells and 133 irregular spatially selective cells were recorded on the track. Linear firing rate maps were calculated for the 3 lighting conditions, plotting the maps with different running direction separately. Figure 9B shows examples of spatially selective neurons with clear firing rate changes between the 3 conditions (l1, l2 and d).

A quantitative analysis of the linear firing rate maps was performed, including only grid cells, border cells and irregular spatially selective cells. Spatial information scores were not significantly different between l1 and l2 conditions (Figure 9C, paired Wilcoxon signed rank test,  $n = 299$  neurons,  $v = 21632$ ,  $p=0.60$ ), but were lower in darkness (l1 vs d,  $v = 34469$ ,  $p<10^{-16}$ ). For most neurons, the location of the firing fields appeared to be preserved across the 3 conditions. Indeed, the median correlation coefficient between linear rate maps of l1 and l2 was 0.92 (Figure 9D). The correlation coefficients were slightly lower between l1 and d (median: 0.81, paired Wilcoxon signed rank test, l1-l2 vs l1-d  $r$  values:  $v = 31909$ ,  $p=10^{-10}$ ). Thus, there was no major reorganization of the firing fields between conditions.

To identify neurons with significant firing rate changes between conditions, a shuffling procedure in which the identity of the conditions was reassigned randomly 500 times was used to obtain chance levels for rate differences. The difference observed at each bin of the linear rate maps was compared to those of the surrogate distribution. Neurons with more than 5 bins in which the observed difference had a probability below 0.01 were considered significant. Approximately half of all recorded neurons showed significant changes between l1 and l2 conditions (245 out of 479, 51.1%). The proportion of neurons with significant rate changes was the same across all functionally defined cell types (Figure 9E,  $\chi^2 = 9.259$ ,  $df = 5$ ,  $p=0.10$ ). When considering only neurons recorded from MEC tetrodes, 35.3% (24 out of 68) of the neurons showed significant differences between l1 and l2 conditions. The percentage of neurons with significant rate changes between l1 and d conditions was 70.8% (339 out of 479) when considering all recorded neurons and 50% (34 out of 68) when limiting the analysis to neurons recorded from MEC tetrodes. These results demonstrate that the firing rate of MEC neurons along the linear track conveys information about distinct nonmetric contextual cues.

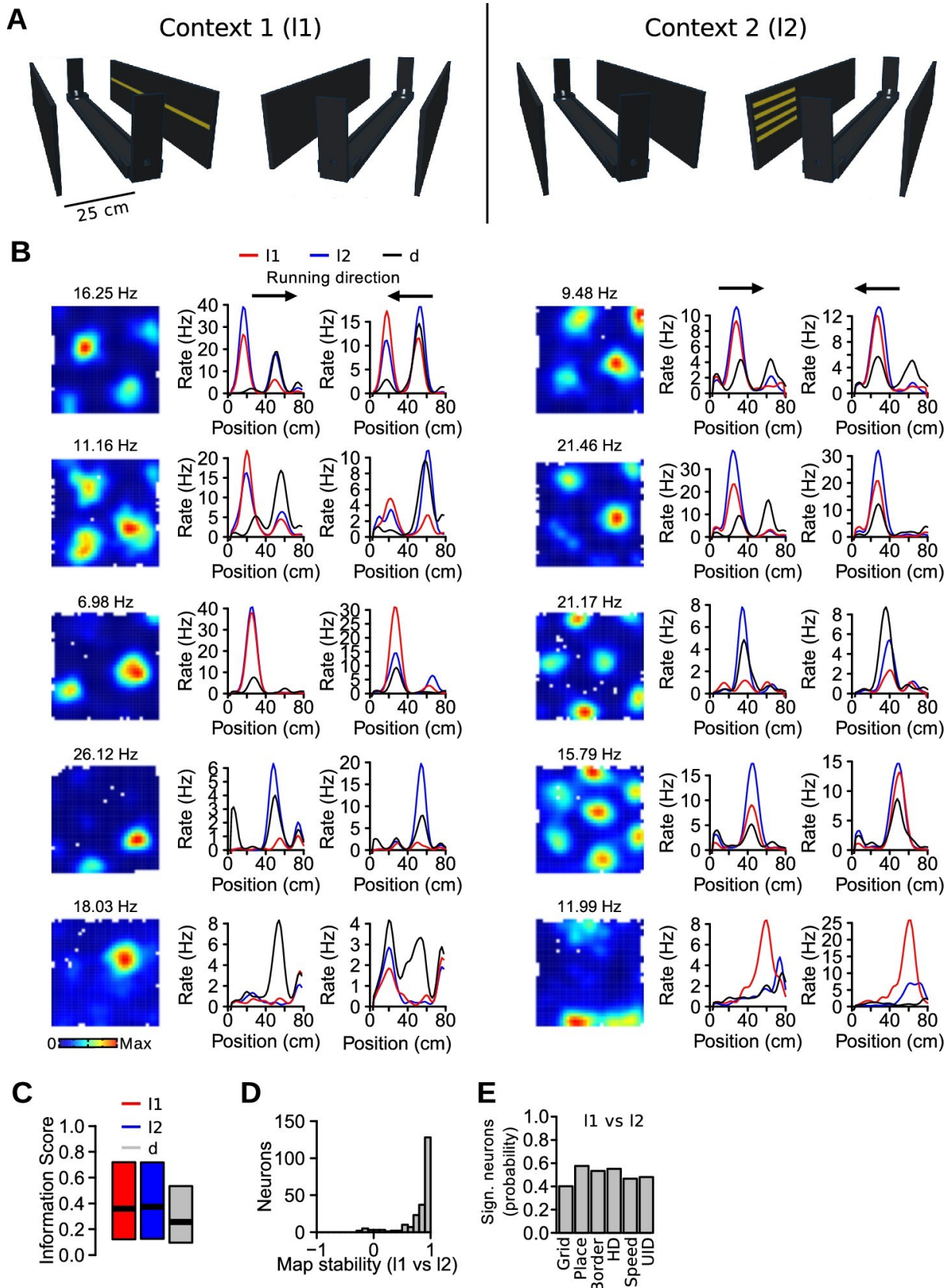


**Figure 9. Nonmetric contextual visual cues affect firing rates of MEC neurons in a 1D environment.** (A) Schematic of the linear track and side walls. The linear track was flanked by two side walls on which LED arrays were attached. In the first context (I1, left), a single row of LEDs on one wall was turned on. In the other context (I2, right), 4 shorter rows of LEDs on the opposite wall were turned on. All LEDs were turned off during dark (d) trials. (B) Example of neurons with firing rate changes between the different conditions. First column, firing rate maps in the square open field. Next two columns, linear

firing rate maps for the 3 conditions, plotted separately for each running direction. Note that the range of the y-axes varies. (C) Spatial information scores (median, first and third quartiles) in the 3 conditions. (D) Stability of linear firing rate maps (correlation coefficient) between l1 and l2 conditions. (E) Proportion of neurons with a significant rate change between l1 and l2 across functionally defined cell types (Grid: grid cells, Place: irregular spatially selective cells, Border: border cells, HD: head-direction cells, Speed: speed-modulated cells, UID: unidentified cells). Taken from Pérez-Escobar et al., (2016b) with kind permission from *eLife Sciences Publications*

## 4. DISCUSSION

This study has aimed to better characterize the effects of visual information on the activity of spatially selective cells in the MEC. The main conclusions that emanate from the results are:

- 1) Visual information is critical for the grid cell firing pattern. Its absence results in its rapid destabilization.
- 2) The speed code of MEC cells depends on visual information.
- 3) Visual information modulates the firing rate of all principal MEC cell types, suggesting heterogeneous information encoding.
- 4) Associating a cognitive ontology (or several) to a cell type, although tempting, may be problematic.

### 4.1 Effects of the removal of visual input on spatially selective cells in the MEC

A few sentences from Pérez-Escobar et al. (2016b) have been paraphrased and integrated into a broader discussion in this section.

The hexagonal firing pattern of grid cells disappears just a few seconds after visual input deprivation, which is at odds with previous findings (Hafting et al., 2005; Allen et al., 2014). There are a few differences between the circular arena experiment and the experimental setups from Hafting et al. (2005) and Allen et al. (2014) that may explain this dissimilitude. First, in the circular arena experiment trials there were two polarizing visual cues (two distinct LED panels) that repeatedly caused reorientations of the MEC spatial representations. In case of uncontrolled cues in the arena (e.g. intra-

trial feces), these would be too unreliable to anchor grid cells, since the changing LED panel orientation overrides them. Second, the circular arena had no walls. This removes potential uncontrolled olfactory and tactile cues. Third, and relatedly to the second point, border cells seem to play an important role in correcting grid cell error accumulation (Hardcastle et al., 2015), but border cells were particularly sensitive to the lack of visual information in the circular arena. A disrupted border cell activity, perhaps due to a lack of uncontrolled wall-related cues, may contribute in turn to the disruption of the hexagonal firing pattern of grid cells. This shows that visual input is much more important for grid cell signal stability than previously thought.

Just when these results were published, another lab reported similar findings: grid cells lose their hexagonal firing pattern seconds after the onset of darkness (Chen et al., 2016). The authors used a standard walled arena and no cue rotations. Since they found a mildly impaired head direction signal but a significantly inaccurate computation of linear displacement, they hypothesize that the cause of the grid cell disruption that they found was caused by the latter factor: the loss of the grid cell firing pattern could be due to a flawed integration of speed information by grid cells. However, in the circular arena experiment, a substantial impairment of the head direction signal was found too. In any case, since grid cells in principle would need to rely on information on both angular direction and speed in order to compute self-motion in the dark, it would only take the disruption of one of the two codes for the grid cell firing pattern to break down.

Moreover, the fact that speed-modulated cells decreased their firing rate in the dark also differs with previous findings. It has been reported that the MEC speed code is context-invariant (Kropff et al., 2015). This was not the case in the circular arena experiment. Self-motion alone did not preserve the speed code. One hypothesis is that optic flow may be needed to preserve it. A modeling study argues for the plausibility of optic flow contributing to grid cell periodicity (Raudies et al., 2012). An explanation for the decreased firing rate of mostly GABAergic speed-modulated cells in the MEC is that cells pre-synaptic to them decreased their firing rate in the dark too. Since speed-

modulated cells have been reported in several brain regions (McNaughton et al., 1983; Saleem et al., 2013; Bender et al., 2015; Fuhrmann et al., 2015), the precise pathways responsible for the speed tuning of MEC cells and whether these signals depend on visual information should be ascertained.

Moreover, in the absence of visual information in the circular arena experiment, a substantial proportion of MEC cells showed different firing rates (usually lower) with respect to lighting conditions. Therefore, the level of activity in the MEC depends on visual input. Of all functional cell types, border cells were the most affected by the loss of visual information, closely followed by head-direction cells. A potential explanation of the lower firing rates of MEC cells in darkness is that afferents from the postrhinal cortex to the MEC conveying visual information to the MEC (Burwell and Amaral, 1998a, 1998b) depolarizing principal neurons (Koganezawa et al., 2015) are less active in the absence of visual input.

## **4.2 Heterogeneous information encoding**

A few sentences from Pérez-Escobar et al. (2016b) have been paraphrased and integrated into a broader discussion in this section.

About half of total cells of all principal cell types showed firing rate changes in response to manipulation of nonmetric contextual cues in the linear track experiment, including grid cells. Therefore, the firing rate of grid cells is context-dependent; grid cells encode contextual information rather than representing an invariant, universal metric of space. The significance of these rate changes is substantial: after the publication of this research, it has been shown that rate changes in MEC neurons, especially after depolarization rather than hyperpolarization, in turn provoke widespread changes in the activity of hippocampal place cells (Kanter et al., 2017). The authors hypothesize that grid cells may convey contextual information to place cells.

Alternatively, since there are reciprocal connections from place to grid cells (Bonnievie et al., 2013), grid cells may inherit contextual information from place cells.

Soon before these results were published, it was suggested that grid cells can encode object information during conditional discrimination tasks (Keene et al., 2016). The results emanating from the linear track experiment are complementary to this, showing that nonmetric contextual manipulations cause grid cell firing rate changes in the absence of behavioral demands: mice did not have to adapt their behavior to contextual changes. Furthermore, it has recently been observed that exploration of different enclosures produces  $\text{Ca}^{2+}$  activity changes MEC Reelin<sup>+</sup> cells (Kitamura et al., 2015). The results here described suggest that some of the context-specific cells of the MEC are indeed classical spatially selective cell types. Moreover, after the publication of these results, the fact that grid cells undergo firing rate alterations and other activity changes in response to nonmetric manipulations has been corroborated by other labs (Diehl et al., 2017; Boccara et al., 2019). See section 4.3 for more literature posterior to the results reported in this dissertation building on this direction.

The precise character of the rate changes of grid cells during 1D navigation in the linear track experiment or when performing memory tasks remains to be further clarified. A likely scenario is that the location of grid firing fields is very stable following contextual changes, and only in-field firing rates are altered. Firing rate changes are common in hippocampal place cells during 2D navigation (Leutgeb et al., 2005) and memory tasks (Lipton et al., 2007; Ferbinteanu et al., 2011; Allen et al., 2012; Ainge et al., 2012). Another possibility is that the firing rate changes observed reflect a shift in the location of the grid firing fields caused by nonmetric contextual cues (Marozzi et al., 2015). If one considers 1D firing maps on the track as slices through the 2D map of the neurons (Yoon et al., 2016), the 1D maps of grid cells in two contexts on the linear track could be considered as slices with different phases or orientations. It is also possible that the contextual cues affect the periodicity of the underlying 2D grid lattice (Krupic et al., 2015; Stensola et al., 2015). While both hypotheses are in principle plausible, the high correlations between the linear firing rate maps in the two contexts

indicate that the change of field location was minimal. Anyway, regardless of the precise underlying mechanisms, the outcome of nonmetric contextual manipulations during 1D navigation is the alteration of the firing rate of grid cells. Therefore, their activity is context-dependent. Grid cells provide information not only about the position of the organism during navigation, but also about the specific context wherein the organism is.

### **4.3 Research building on the effects of visual landmarks and context-specificity of grid cell activity shown in this work**

Before I discuss the implications of these results on behavior (path integration) and cognitive representations in sections 4.4 and 4.5 respectively, I discuss the reception of my work since its publication and related posterior findings.

First, some studies have corroborated and further qualified non-metric codes in grid cell activity. Diehl et al. (2017) have shown that grid and other spatially selective MEC cells respond to changes of environmental features (in the case of grid cells this is manifested as firing rate changes, in consonance with my results). Similarly, Ismakov et al. (2017) have reported that the peak field firing rate distribution of grid cells remaps after context change. Aronov et al. (2017) have discovered that the activity of some grid cells is modulated by task-dependent auditory frequencies. Chen et al. (2019) have shown that the activity of grid cells responds to environmental cues, albeit less than place cells. Cholvin, Hainmueller and Bartos (2021) have observed that MEC boutons with a grid-like firing activity convey contextual information to the hippocampus, where this information becomes more reliable. Some have suggested that grid cells may play a role in the organization of general, conceptual knowledge and concept learning (Constantinescu, O'Reilly and Behrens, 2016; Mok and Love, 2019; note that the latter suggest that grid cell activity does not constitute representations but a mechanism for error monitoring of hippocampal

representations). It has also been found that grid cell activity encodes spatial information beyond the intrinsic metric properties of an environment, like combinations of several cues (Hardcastle et al., 2017) and the location of goals (Boccaro et al., 2019; Butler, Hardcastle and Giocomo, 2019). Last, an interesting study by Dannenberg et al. (2020) provides an alternative explanation to the conclusions that I draw in this dissertation and in Pérez-Escobar et al. (2016b) that the firing rates of MEC neurons is higher during light conditions than in darkness, and that it encodes non-metric properties of the environment. Dannenberg et al. show that non-informative light projected to the retina increases the firing rates of MEC neurons and argue that this is enough to account for the different firing rates in light and dark conditions. However, I have also shown that the firing rates of MEC neurons, including grid cells, are different across two different light conditions, which makes it implausible that non-informative light is the only factor accounting for firing rate differences.

Second, more studies have investigated the effect of visual landmarks on the spatial code of the MEC. Savelli, Luck and Knierim (2017) have provided further evidence of the effect of visual cues outside the metric space on grid cells: the grid pattern does not adjust properly to rotation of the metric arena when this rotation conflicts with cues outside the metric boundaries. Furthermore, it has been shown that MEC cells encode spatial cues (Kinkhabwala et al., 2020); it is possible that these cells, also known as cue cells, project to grid cells, thereby correcting error accumulation similarly to border cells. The result reported in this dissertation that grid cells require visual landmarks to preserve their grid firing pattern has been hypothesized to account for the discovery that some head-direction cells are driven by visual landmarks instead of being merely anchored to them (Kornienko et al., 2018).

## 4.4 Path integration and representationalism

As discussed in the introduction, the fact that environmental boundaries can alter grid cell periodicity raised doubt on whether grid cells encoded a universal metric of space and played a substantial role in path integration. The fact that grid cells change their firing rate in response to contextual manipulations may be interpreted as further challenging these notions as well. However, as I pointed out in section 1.2 of the introduction, cognitive representation and behavioral function are issues that, while finding confluence points and overlapping to some degree, deserve their own individual treatments. In fact, as we saw, representationalism could be dropped altogether, and that would not necessarily preclude the search for neuronal bases of behavior: an alternative approach would account for the relationship between neuronal substrata and overt behavior. What representationalism does is assisting with making inferences about the roles of substrata in behavior. For instance, that a given substrate represents  $A$  instead of  $A'$  may lead to the inference that it is involved in behavior  $B$  instead of behavior  $B'$ , without getting into the material details. This may be useful, but we should not lose sight of what representationalism is from a practical perspective: a convenient approach filling explanatory gaps in what would otherwise be a materialistic and mechanistic approach (currently the gold standard in other scientific fields). In a strictly materialistic and mechanistic approach, when the gap is bridged (or almost bridged), some say that representations become at best redundant (Piccinini and Craver, 2011), and if we decide to commit to materialism in a metaphysically strong sense, misleading. This is a clarification on common views about scientific practices and metaphysical notions, not my own take on the metaphysical character of nature – which may or may not be dualistic, and which does not matter in this context.

Be it as it may, this clarification on representationalism in cognitive neuroscience is useful to understand the following: if we understand representations heuristically, as bridges closing explanatory gaps, we must be aware of both the heuristic value of the approach and its limitations. One of the limitations is that the bridging may not be

entirely accurate. For this reason, even if we commit to representationalism and find that grid cells do not represent an invariant, universal metric of space, but instead their activity does not fit a readily intuitive category, grid cells may still be functionally related to certain behavioral functions like path integration – they may just not be the sole substrate implicated, and they may be implicated in other behaviors too. Moreover, the conclusion that grid cells encode heterogeneous information implicitly relies on intuitive categories themselves: one says that the information is “heterogeneous” or “multimodal” because it does not adjust to any pure category already available to us (like Euclidian space from elemental mathematics, or artifacts like maps, compasses, and so forth).

Indeed, recent studies have provided evidence that grid cells are functionally related to path integration. Grid cell spatial selectivity correlates with integrated distance in rats and humans (Chen et al., 2015; Jacob et al., 2019). Moreover, a recent study removed NMDA receptors from retro-hippocampal regions of mice, achieving a selective disruption of grid cell activity in the form of lower grid periodicity and spatial selectivity while sparing head direction, border, and speed signals (Gil et al., 2018). The authors found that this selective disruption is linked to impaired path integration performance. However, all things considered, the fact that grid cells seem to be needed for path integration does not necessarily entail that they represent a universal metric of space, or even that they represent at all for that matter.

#### **4.5 Alternative takes on representations**

It was initially thought that place cells provided a pure spatial signal, but eventually they were shown to encode heterogeneous information, mixing spatial, goal and context information (see Mallory and Giocomo [2018] for a review). The hope of finding a universal metric of space did not die, and potential neurobiological substrata were traced back to the MEC (the main source of cortical input to the hippocampus). However, we have seen that multimodal information is already present in the MEC.

There is nothing wrong with certain approaches or “hopes” (in the form of given cognitive ontologies or representationalism in general) as long as the hope in question turns out to be pragmatic, yielding concrete useful insights and discoveries: they may go perpetually unfulfilled, or tautologically self-fulfilled, but still, they may lead to useful insights and findings (in this case, that certain neurobiological substrata are related to path integration).

However, I want to make the point that, at the very least, alternative possibilities should be considered. Metaphysics aside, just like the transition from behaviorism to cognitivism happened on pragmatic grounds – it turned out to be useful because it provided easy explanations of complex behavior – potential further reframings should be considered on similar grounds at any given point. In fact, the very pragmatic value of hopes, intuitions and strategies may be compromised if they are mistaken for something else – for instance, truth factories by epistemic virtue. There are at least four alternatives worth considering:

1) Investigating alternative coding strategies without a substantial modification of spatial cognitive ontologies. This option has been chosen by recent mainstream literature in cognitive neuroscience aiming to refine the cognitive representations at stake (Hardcastle et al., 2017; Bellmund et al., 2018; Grieves, Duvelle and Dudchenko, 2018; Mok and Love, 2019; Rodríguez-Domínguez and Caplan, 2019; Chen et al., 2019; Han, Wu and Lai, 2020; Keinath et al., 2020; Taube and Shinder, 2020; Vandrey, Duncan and Ainge, 2021; Tennant et al., 2022). It is worth noting that some more exotic options, like embodied cognition, have been explored in philosophy and science, but I will not review them here.

2) Casting doubt on intuitive cognitive ontologies, while staying committed to representationalism. The idea that the brain is bound by our cognitive ontologies of preference should be contested. It could be argued that individual cells or broader brain processes align with our categories, because concepts and ideas emerge from the brain as well: if the brain processes information and this in turn determines how we perceive the world, it could be the case that our cognitive ontologies align with the

brain. In a sense, this would be the biggest hope of someone trying to naturalize Kant's pure intuition. Furthermore, the cross-cultural prevalence of spatial – although heterogeneous – concepts seems to support this idea. However, this does not confirm that we speak of space because we “process space”, rather than we look for spatial information in the brain because we happen to speak of space. If that was the case, every other type of concept we use would be subjected to the same treatment. However, some concepts overlap, and others do not exist harmonically with each other. Furthermore, cognitive ontologies come to be and disappear across time, while brains remain relatively stable. Last, most cognitive ontologies are not shared across cultures either. Therefore, the view that the brain is subjected to spatial cognitive ontologies should be contested at least on metaphysical grounds. In principle, there is no reason to hold the belief that the brain must respect our commonsense intuitions. It has been suggested that the fact that mainstream cognitive neuroscience adheres to intuitive categories like time, space and numerosity is due to the relatively young age and lack of maturity of the discipline (Buetti and Walsh, 2009). In a more general direction, it has been argued that some coding strategies considered in the scientific practice have been influenced by artifact analogies more than just heuristically (Pérez-Escobar, 2020), and that artifact analogies have important limitations in biology (Nicholson, 2012; Nicholson, 2013; Nicholson, 2014). Therefore, this strategy would benefit from constant skepticism and pragmatism on the selected cognitive ontologies.

3) Adopting a deflationary perspective on representationalism. Philosopher of cognitive science Frances Egan has extensively argued that most cognitive ontologies are useful fictions that help us make sense of brain processes (Egan, 2014; Egan, 2017; Egan, 2019; Egan, 2020). However, she does not discard representationalism altogether, as she argues that there are fundamental mathematical relations between components (cells, ensembles) governing information processing in the brain. While intuitive cognitive ontologies are merely a heuristic “gloss” over computation in her view – which does not mean they should be readily discarded – mathematics may describe real brain dynamics. However, this approach requires caution: as I have noted elsewhere (Pérez-Escobar, 2020) some mathematical descriptions emerge from artifact

analogies (for instance, analogies between a compass and head-direction cells) and are in practice configured to depend on and promote the use of cognitive ontologies via epistemic circularity and teleological explanations. The presence of mathematical computations does not imply the absence of cognitive representations, and often, they are presented as an overall package. This may happen because, among other reasons, mathematical models may act not as descriptions but as rules on how phenomena ought to be described (Pérez-Escobar, 2022).

4) Doing without representationalism altogether (eliminativism/physical reductionism). Since cognitive neuroscientists often treat representations, including spatial representations, as substantial – rather than heuristic – elements of their research programs (Sullivan, 2010a; Sullivan, 2010b), this approach requires a major overhaul of the discipline.

I want to stress again that, while this can be understood as a metaphysical issue or a matter of truth or falsity (Ramsey, 2020), it would be wise to pay attention to the history of science in general (for the classical work on scientific revolutions: Kuhn, 1962; for the argument that there is no such thing as *the* scientific method: Feyerabend, 1975) and the history of cognitivism in particular (as outlined in this work), and see it as a pragmatic matter instead: one about seeing how far the view that the brain processes spatial information in a certain way (or information at all) takes us, compared to the alternatives (for a recent, broader defense of content pragmatism, see Coelho Mollo, [2020]). After all, our commitments of this kind provide a frame for the truths we subsequently find (and vice versa). Just like the cognitive revolution came to reframe important theoretical issues when it was deemed appropriate to transcend behaviorism, we should be ready to evaluate the need for revisionary work on the foundations of cognitive neuroscience and representationalism in particular when/if the time is due.

## 5. SUMMARY

This work has investigated the activity of spatially selective neurons in the medial entorhinal cortex following manipulations of non-metric properties of the environment. The types of neurons investigated were head-direction cells, border cells, speed cells, and especially, grid cells. The latter type of cells is thought to encode a universal Euclidian metric of space and be the main neurobiological substrata for path integration.

The main findings are: 1) The removal of visual landmarks caused the grid cell and head-direction cell signals to break down, the speed code to change, and the border cell activity to be less confined to the borders of the arena, and 2) the manipulation of non-metric, visual features of the environment affected the firing rate code of grid cells, head-direction cells, border cells and speed cells, thus revealing the context specificity of their activity.

Because of such a context specificity, these findings argue against the notion that grid cells act as the neurobiological substratum of a cognitive representation of a universal Euclidian metric of space. A similar conclusion holds for other cell types. In turn, these results raise doubt about the possibility of ascribing intuitive spatial categories (maps, compasses, speedometers...) to specific cell types in a way that the brain and our intuitions display similar conceptual structures. However, this does not undermine the possibility that certain cell types may play prominent roles in behaviors like path integration; instead, it suggests a much more complicated functional role than what our heuristic spatial intuitions may capture.

## 6. ZUSAMMENFASSUNG

In dieser Arbeit wurde die Aktivität räumlich selektiver Neuronen im medialen entorhinalen Kortex nach Manipulationen nicht-metrischer Eigenschaften der Umgebung untersucht. Bei den untersuchten Neuronen handelte es sich um Kopfrichtungszellen, Randzellen, Geschwindigkeitszellen und insbesondere um Gitterzellen. Es wird angenommen, dass der letztgenannte Zelltyp eine universelle euklidische Metrik des Raums kodiert und das wichtigste neurobiologische Substrat für die Pfadintegration darstellt.

Die wichtigsten Ergebnisse sind: 1) Die Entfernung visueller Orientierungspunkte führte dazu, dass die Signale der Gitterzellen und der Kopf-Richtungs-Zellen zusammenbrachen, sich der Geschwindigkeitscode änderte und die Aktivität der Randzellen weniger auf die Grenzen der Arena beschränkt war, und 2) die Manipulation nicht-metrischer, visueller Merkmale der Umgebung wirkte sich auf den Feuerratencode der Gitterzellen, der Kopf-Richtungs-Zellen, der Randzellen und der Geschwindigkeitszellen aus, wodurch die Kontextspezifität ihrer Aktivität deutlich wurde.

Aufgrund dieser Kontextspezifität sprechen diese Befunde gegen die Vorstellung, dass Gitterzellen als neurobiologisches Substrat einer kognitiven Repräsentation einer universellen euklidischen Metrik des Raums fungieren. Eine ähnliche Schlussfolgerung gilt auch für andere Zelltypen. Diese Ergebnisse lassen wiederum Zweifel an der Möglichkeit aufkommen, intuitive räumliche Kategorien (Karten, Kompass, Geschwindigkeitsmesser...) bestimmten Zelltypen zuzuordnen, so dass das Gehirn und unsere Intuitionen ähnliche konzeptuelle Strukturen aufweisen. Dies untergräbt jedoch nicht die Möglichkeit, dass bestimmte Zelltypen eine herausragende Rolle bei Verhaltensweisen wie der Pfadintegration spielen; es deutet vielmehr auf eine viel kompliziertere funktionelle Rolle hin, als sie unsere heuristischen räumlichen Intuitionen erfassen können.

## 7. REFERENCES

- Ainge, J. A., Tamosiunaite, M., Wörgötter, F., & Dudchenko, P. A. (2012). Hippocampal place cells encode intended destination, and not a discriminative stimulus, in a conditional T-maze task. *Hippocampus*, 22(3), 534-543.
- Allen, K., Rawlins, J. N. P., Bannerman, D. M., & Csicsvari, J. (2012). Hippocampal place cells can encode multiple trial-dependent features through rate remapping. *Journal of Neuroscience*, 32(42), 14752-14766.
- Allen, K., Gil, M., Resnik, E., Toader, O., Seeburg, P., & Monyer, H. (2014). Impaired path integration and grid cell spatial periodicity in mice lacking GluA1-containing AMPA receptors. *Journal of Neuroscience*, 34(18), 6245-6259.
- Aronov, D., Nevers, R., & Tank, D. W. (2017). Mapping of a non-spatial dimension by the hippocampal-entorhinal circuit. *Nature*, 543(7647), 719-722.
- Barry, C., Lever, C., Hayman, R., Hartley, T., Burton, S., O'Keefe, J., ... & Burgess, N. (2006). The boundary vector cell model of place cell firing and spatial memory. *Reviews in the Neurosciences*, 17(1-2), 71.
- Barry, C., Hayman, R., Burgess, N., & Jeffery, K. J. (2007). Experience-dependent rescaling of entorhinal grids. *Nature neuroscience*, 10(6), 682-684.
- Bellmund, J. L., Gärdenfors, P., Moser, E. I., & Doeller, C. F. (2018). Navigating cognition: Spatial codes for human thinking. *Science*, 362(6415), eaat6766.
- Bender, F., Gorbati, M., Cadavieco, M. C., Denisova, N., Gao, X., Holman, C., ... & Ponomarenko, A. (2015). Theta oscillations regulate the speed of locomotion via a hippocampus to lateral septum pathway. *Nature communications*, 6(1), 1-11.
- Bennett, A. T. (1996). Do animals have cognitive maps?. *Journal of Experimental Biology*, 199(1), 219-224.
- Boccaro, C. N., Sargolini, F., Thoresen, V. H., Solstad, T., Witter, M. P., Moser, E. I., & Moser, M. B. (2010). Grid cells in pre-and parasubiculum. *Nature neuroscience*, 13(8), 987-994.

- Boccaro, C. N., Nardin, M., Stella, F., O'Neill, J., & Csicsvari, J. (2019). The entorhinal cognitive map is attracted to goals. *Science*, 363(6434), 1443-1447.
- Bonnevie, T., Dunn, B., Fyhn, M., Hafting, T., Derdikman, D., Kubie, J. L., ... & Moser, M. B. (2013). Grid cells require excitatory drive from the hippocampus. *Nature neuroscience*, 16(3), 309-317.
- Bostock, E., Muller, R. U., & Kubie, J. L. (1991). Experience-dependent modifications of hippocampal place cell firing. *Hippocampus*, 1(2), 193-205.
- Buetfering, C., Allen, K., & Monyer, H. (2014). Parvalbumin interneurons provide grid cell-driven recurrent inhibition in the medial entorhinal cortex. *Nature neuroscience*, 17(5), 710-718.
- Bueti, D., & Walsh, V. (2009). The parietal cortex and the representation of time, space, number and other magnitudes. *Philosophical Transactions of the Royal Society of London B: Biological Sciences*, 364(1525), 1831-1840.
- Burak, Y., & Fiete, I. R. (2009). Accurate path integration in continuous attractor network models of grid cells. *PLoS Comput Biol*, 5(2), e1000291.
- Burgess, N., Barry, C., & O'Keefe, J. (2007). An oscillatory interference model of grid cell firing. *Hippocampus*, 17(9), 801-812.
- Burwell, R. D., & Amaral, D. G. (1998). Cortical afferents of the perirhinal, postrhinal, and entorhinal cortices of the rat. *Journal of comparative neurology*, 398(2), 179-205.
- Burwell, R. D., & Amaral, D. G. (1998). Perirhinal and postrhinal cortices of the rat: interconnectivity and connections with the entorhinal cortex. *Journal of Comparative Neurology*, 391(3), 293-321.
- Butler, W. N., Smith, K. S., van der Meer, M. A., & Taube, J. S. (2017). The head-direction signal plays a functional role as a neural compass during navigation. *Current Biology*, 27(9), 1259-1267.
- Chen, L. L., Lin, L. H., Green, E. J., Barnes, C. A., & McNaughton, B. L. (1994). Head-direction cells in the rat posterior cortex. *Experimental brain research*, 101(1), 8-23.

- Chen, X., He, Q., Kelly, J. W., Fiete, I. R., & McNamara, T. P. (2015). Bias in human path integration is predicted by properties of grid cells. *Current Biology*, 25(13), 1771-1776.
- Chen, G., Manson, D., Cacucci, F., & Wills, T. J. (2016). Absence of visual input results in the disruption of grid cell firing in the mouse. *Current Biology*, 26(17), 2335-2342.
- Chen, G., Lu, Y., King, J. A., Cacucci, F., & Burgess, N. (2019). Differential influences of environment and self-motion on place and grid cell firing. *Nature communications*, 10(1), 630.
- Cholvin, T., Hainmueller, T., & Bartos, M. (2021). The hippocampus converts dynamic entorhinal inputs into stable spatial maps. *Neuron*, 109(19), 3135-3148.
- Chomsky, N. (1955) *The logical structure of linguistic theory*. Unpublished manuscript; revised in 1956 and distributed from MIT Library; published with some abridgement in 1975 by Plenum Press, New York.
- Chomsky, N. (1959). On certain formal properties of grammars. *Information and Control*, 1, 91-112.
- Chomsky N. (1962). Explanatory models in linguistics. In Nagel E., Suppes P., Tarski A. (Eds.) *Logic, Methodology, and Philosophy of Science*, pp. 528-550. Stanford, CA: Stanford University Press.
- Coehlo Mollo, D. (2020). Content Pragmatism Defended. *Topoi*, 39, 103-113.
- Collett, M., Chittka, L., & Collett, T. S. (2013). Spatial memory in insect navigation. *Current Biology*, 23(17), R789-R800.
- Constantinescu, A. O., O'Reilly, J. X., & Behrens, T. E. (2016). Organizing conceptual knowledge in humans with a gridlike code. *Science*, 352(6292), 1464-1468.
- Copeland, B. J. and O. Shagrir (2013). Turing versus Godel on computability and the mind. In *Computability: Turing, Godel, Church, and Beyond*, 1-33. MIT Press.
- Couey, J. J., Witoelar, A., Zhang, S. J., Zheng, K., Ye, J., Dunn, B., ... & Witter, M. P. (2013). Recurrent inhibitory circuitry as a mechanism for grid formation. *Nature neuroscience*, 16(3), 318-324.

Csicsvari, J., Hirase, H., Czurko, A., & Buzsáki, G. (1998). Reliability and state dependence of pyramidal cell–interneuron synapses in the hippocampus: an ensemble approach in the behaving rat. *Neuron*, 21(1), 179-189.

Dannenberg, H., Lazaro, H., Nambiar, P., Hoyland, A., & Hasselmo, M. E. (2020). Effects of visual inputs on neural dynamics for coding of location and running speed in medial entorhinal cortex. *Elife*, 9, e62500.

Diehl, G. W., Hon, O. J., Leutgeb, S., & Leutgeb, J. K. (2017). Grid and nongrid cells in medial entorhinal cortex represent spatial location and environmental features with complementary coding schemes. *Neuron*, 94(1), 83-92.

Egan, F. (2014). How to Think about Mental Content. *Philosophical Studies* 170, 115- 135.

Egan, F. (2017). Function-Theoretic Explanation and the Search for Neural Mechanisms. In *Explanation and Integration in Mind and Brain Science*, D. M. Kaplan (Ed.). Oxford University Press.

Egan, F. (2019). The Nature and Function of Content in Computational Models. In *The Routledge Handbook of the Computational Mind*. Routledge, Abingdon.

Egan, F. (2020). A Deflationary Account of Mental Representation. In *Mental Representations*, J. Smortchkova, K. Dolega and T. Schlicht (Eds.). Oxford University Press.

Etienne, A. S., Maurer, R., & Séguinot, V. (1996). Path integration in mammals and its interaction with visual landmarks. *Journal of Experimental Biology*, 199(1), 201-209.

Etienne, A. S., Boulens, V., Maurer, R., Rowe, T., & Siegrist, C. (2000). A brief view of known landmarks reorientates path integration in hamsters. *Naturwissenschaften*, 87(11), 494-498.

Etienne, A. S., Maurer, R., Boulens, V., Levy, A., & Rowe, T. (2004). Resetting the path integrator: a basic condition for route-based navigation. *Journal of Experimental Biology*, 207(9), 1491-1508.

- Evans, T., Bicanski, A., Bush, D., & Burgess, N. (2016). How environment and self-motion combine in neural representations of space. *The Journal of physiology*, 594(22), 6535-6546.
- Ferbinteanu, J., Shirvalkar, P., & Shapiro, M. L. (2011). Memory modulates journey-dependent coding in the rat hippocampus. *Journal of Neuroscience*, 31(25), 9135-9146.
- Feyerabend, P. (1975). *Against Method: Outline of an Anarchist Theory of Knowledge*. London: New Left Books.
- Fuhs, M. C., & Touretzky, D. S. (2006). A spin glass model of path integration in rat medial entorhinal cortex. *Journal of Neuroscience*, 26(16), 4266-4276.
- Fuhrmann, F., Justus, D., Sosulina, L., Kaneko, H., Beutel, T., Friedrichs, D., ... & Remy, S. (2015). Locomotion, theta oscillations, and the speed-correlated firing of hippocampal neurons are controlled by a medial septal glutamatergic circuit. *Neuron*, 86(5), 1253-1264.
- Fyhn, M., Hafting, T., Treves, A., Moser, M. B., & Moser, E. I. (2007). Hippocampal remapping and grid realignment in entorhinal cortex. *Nature*, 446(7132), 190-194.
- Fyhn, M., Hafting, T., Witter, M. P., Moser, E. I., & Moser, M. B. (2008). Grid cells in mice. *Hippocampus*, 18(12), 1230-1238.
- Gerrans, P. (2014). *The Measure of Madness*. MIT Press.
- Gil, M., Ancau, M., Schlesiger, M. I., Neitz, A., Allen, K., De Marco, R. J., & Monyer, H. (2018). Impaired path integration in mice with disrupted grid cell firing. *Nature neuroscience*, 21(1), 81-91.
- Goodridge, J. P., & Taube, J. S. (1995). Preferential use of the landmark navigational system by head direction cells in rats. *Behavioral neuroscience*, 109(1), 49.
- Görner, P. (1958). Die optische und kinästhetische Orientierung der Trichterspinn Agelena Labyrinthica (C1.). *Zeitschrift für vergleichende Physiologie*, 41(2), 111-153.
- Grievess, R. M., Duvelle, É., & Dudchenko, P. A. (2018). A boundary vector cell model of place field repetition. *Spatial Cognition & Computation*, 18(3), 217-256.

- Hafting, T., Fyhn, M., Molden, S., Moser, M. B., & Moser, E. I. (2005). Microstructure of a spatial map in the entorhinal cortex. *Nature*, *436*(7052), 801-806.
- Han, K., Wu, D., & Lai, L. (2020). A Brain-Inspired Adaptive Space Representation Model Based on Grid Cells and Place Cells. *Computational Intelligence and Neuroscience*, 2020.
- Hardcastle, K., Ganguli, S., & Giocomo, L. M. (2015). Environmental boundaries as an error correction mechanism for grid cells. *Neuron*, *86*(3), 827-839.
- Hardcastle, K., Maheswaranathan, N., Ganguli, S., & Giocomo, L. M. (2017). A multiplexed, heterogeneous, and adaptive code for navigation in medial entorhinal cortex. *Neuron*, *94*(2), 375-387.
- Ismakov, R., Barak, O., Jeffery, K., & Derdikman, D. (2017). Grid cells encode local positional information. *Current Biology*, *27*(15), 2337-2343.
- Jacob, P. Y., Capitano, F., Poucet, B., Save, E., & Sargolini, F. (2019). Path integration maintains spatial periodicity of grid cell firing in a 1D circular track. *Nature communications*, *10*(1), 1-13.
- Jander, R. (1957). Die optische Richtungsorientierung der Roten Waldameise (*Formica rufa* L.). *Zeitschrift für vergleichende Physiologie*, *40*(2), 162-238.
- Jankowski, M. M., Islam, M. N., Wright, N. F., Vann, S. D., Erichsen, J. T., Aggleton, J. P., & O'Mara, S. M. (2014). Nucleus reuniens of the thalamus contains head direction cells. *Elife*, *3*, e03075.
- Kanter, B. R., Lykken, C. M., Avesar, D., Weible, A., Dickinson, J., Dunn, B., ... & Kentros, C. G. (2017). A novel mechanism for the grid-to-place cell transformation revealed by transgenic depolarization of medial entorhinal cortex layer II. *Neuron*, *93*(6), 1480-1492.
- Keene, C. S., Bladon, J., McKenzie, S., Liu, C. D., O'Keefe, J., & Eichenbaum, H. (2016). Complementary functional organization of neuronal activity patterns in the perirhinal, lateral entorhinal, and medial entorhinal cortices. *Journal of Neuroscience*, *36*(13), 3660-3675.

- Keinath, A. T., Rechnitz, O., Balasubramanian, V., & Epstein, R. A. (2021). Environmental deformations dynamically shift human spatial memory. *Hippocampus*, *31*(1), 89-101.
- Kinkhabwala, A. A., Gu, Y., Aronov, D., & Tank, D. W. (2020). Visual cue-related activity of cells in the medial entorhinal cortex during navigation in virtual reality. *Elife*, *9*, e43140.
- Kitamura, T., Sun, C., Martin, J., Kitch, L. J., Schnitzer, M. J., & Tonegawa, S. (2015). Entorhinal cortical ocean cells encode specific contexts and drive context-specific fear memory. *Neuron*, *87*(6), 1317-1331.
- Knierim, J. J., Kudrimoti, H. S., & McNaughton, B. L. (1995). Place cells, head direction cells, and the learning of landmark stability. *Journal of Neuroscience*, *15*(3), 1648-1659.
- Koganezawa, N., Gisetstad, R., Husby, E., Doan, T. P., & Witter, M. P. (2015). Excitatory postrhinal projections to principal cells in the medial entorhinal cortex. *Journal of Neuroscience*, *35*(48), 15860-15874.
- Kornienko, O., Latuske, P., Bassler, M., Kohler, L., & Allen, K. (2018). Non-rhythmic head-direction cells in the parahippocampal region are not constrained by attractor network dynamics. *Elife*, *7*, e35949.
- Kriegeskorte, N., & Douglas, P. K. (2018). Cognitive computational neuroscience. *Nature neuroscience*, *21*(9), 1148-1160.
- Kropff, E., Carmichael, J. E., Moser, M. B., & Moser, E. I. (2015). Speed cells in the medial entorhinal cortex. *Nature*, *523*(7561), 419-424.
- Krupic, J., Bauza, M., Burton, S., Barry, C., & O'Keefe, J. (2015). Grid cell symmetry is shaped by environmental geometry. *Nature*, *518*(7538), 232-235.
- Krupic, J., Bauza, M., Burton, S., & O'Keefe, J. (2018). Local transformations of the hippocampal cognitive map. *Science*, *359*(6380), 1143-1146.
- Kuhn, T. S. (1962). *The structure of scientific revolutions*. University of Chicago press.

Latuske, P., Toader, O., & Allen, K. (2015). Interspike intervals reveal functionally distinct cell populations in the medial entorhinal cortex. *Journal of Neuroscience*, *35*(31), 10963-10976.

Leutgeb, S., Leutgeb, J. K., Moser, M. B., & Moser, E. I. (2005). Place cells, spatial maps and the population code for memory. *Current opinion in neurobiology*, *15*(6), 738-746.

Lever, C., Burton, S., Jeewajee, A., O'Keefe, J., & Burgess, N. (2009). Boundary vector cells in the subiculum of the hippocampal formation. *Journal of Neuroscience*, *29*(31), 9771-9777.

Lipton, P. A., White, J. A., & Eichenbaum, H. (2007). Disambiguation of overlapping experiences by neurons in the medial entorhinal cortex. *Journal of Neuroscience*, *27*(21), 5787-5795.

Maguire, E. A., Gadian, D. G., Johnsrude, I. S., Good, C. D., Ashburner, J., Frackowiak, R. S., & Frith, C. D. (2000). Navigation-related structural change in the hippocampi of taxi drivers. *Proceedings of the National Academy of Sciences*, *97*(8), 4398-4403.

Maguire, E. A., Woollett, K., & Spiers, H. J. (2006). London taxi drivers and bus drivers: a structural MRI and neuropsychological analysis. *Hippocampus*, *16*(12), 1091-1101.

Mallory, C. S., & Giocomo, L. M. (2018). Heterogeneity in hippocampal place coding. *Current opinion in neurobiology*, *49*, 158-167.

Marozzi, E., Ginzberg, L. L., Alenda, A., & Jeffery, K. J. (2015). Purely translational realignment in grid cell firing patterns following nonmetric context change. *Cerebral Cortex*, *25*(11), 4619-4627.

Marshall, L., Henze, D. A., Hirase, H., Leinekugel, X., Dragoi, G., & Buzsáki, G. (2002). Hippocampal pyramidal cell-interneuron spike transmission is frequency dependent and responsible for place modulation of interneuron discharge. *Journal of Neuroscience*, *22*(2), RC197.

Maurer, A. P., Cowen, S. L., Burke, S. N., Barnes, C. A., & McNaughton, B. L. (2006). Phase precession in hippocampal interneurons showing strong functional coupling to individual pyramidal cells. *Journal of Neuroscience*, *26*(52), 13485-13492.

- McNaughton, B. L., Barnes, C. A., & O'Keefe, J. J. E. B. R. (1983). The contributions of position, direction, and velocity to single unit activity in the hippocampus of freely-moving rats. *Experimental brain research*, 52(1), 41-49.
- McNaughton, B. L., Barnes, C. A., Gerrard, J. L., Gothard, K., Jung, M. W., Knierim, J. J., ... & Weaver, K. L. (1996). Deciphering the hippocampal polyglot: the hippocampus as a path integration system. *Journal of Experimental Biology*, 199(1), 173-185.
- McNaughton, B. L., Battaglia, F. P., Jensen, O., Moser, E. I., & Moser, M. B. (2006). Path integration and the neural basis of the 'cognitive map'. *Nature Reviews Neuroscience*, 7(8), 663-678.
- Miller, G. A. (1956). The magical number seven, plus or minus two: Some limits on our capacity for processing information. *Psychological review*, 63(2), 81.
- Mittelstaedt, M. L., & Mittelstaedt, H. (1980). Homing by path integration in a mammal. *Die Naturwissenschaften*, 67(11), 566-567.
- Mizuseki, K., Sirota, A., Pastalkova, E., & Buzsáki, G. (2009). Theta oscillations provide temporal windows for local circuit computation in the entorhinal-hippocampal loop. *Neuron*, 64(2), 267-280.
- Mok, R. M., & Love, B. C. (2019). A non-spatial account of place and grid cells based on clustering models of concept learning. *Nature communications*, 10(1), 1-9.
- Moser, E. I., & Moser, M. B. (2008). A metric for space. *Hippocampus*, 18(12), 1142-1156.
- Morris, R. G. (1981). Spatial localization does not require the presence of local cues. *Learning and motivation*, 12(2), 239-260.
- Muller, R. U., & Kubie, J. L. (1987). The effects of changes in the environment on the spatial firing of hippocampal complex-spike cells. *Journal of Neuroscience*, 7(7), 1951-1968.
- Müller, M., & Wehner, R. (1988). Path integration in desert ants, *Cataglyphis fortis*. *Proceedings of the National Academy of Sciences*, 85(14), 5287-5290.

- Nicholson, D. J. (2012). The concept of mechanism in biology. *Studies in History and Philosophy of Science Part C: Studies in History and Philosophy of Biological and Biomedical Sciences*, 43(1), 152-163.
- Nicholson, D. J. (2013). Organisms≠ machines. *Studies in History and Philosophy of Science Part C: Studies in History and Philosophy of Biological and Biomedical Sciences*, 44(4), 669-678.
- Nicholson, D. J. (2014). The machine conception of the organism in development and evolution: A critical analysis. *Studies in History and Philosophy of Science Part C: Studies in History and Philosophy of Biological and Biomedical Sciences*, 48, 162-174
- O'Keefe, J., Dostrovsky, J. (1971). The hippocampus as a spatial map. Preliminary evidence from unit activity in the freely-moving rat. *Brain Research*, 34, 171-175.
- O'Keefe, J. (1976). Place units in the hippocampus of the freely moving rat. *Experimental neurology*, 51(1), 78-109.
- O'Keefe, J., & Nadel, L. (1978). *The hippocampus as a cognitive map*. Clarendon Press.
- Olton, D. S., & Samuelson, R. J. (1976). Remembrance of places past: Spatial discrimination and response inhibition. *Journal of Experimental Psychology: Animal Behavior Processes*, 2, 97-116.
- Pastoll, H., Solanka, L., van Rossum, M. C., & Nolan, M. F. (2013). Feedback inhibition enables theta-nested gamma oscillations and grid firing fields. *Neuron*, 77(1), 141-154.
- Pérez-Escobar, J. A., Kornienko, O., Latuske, P., Kohler, L., & Allen, K. (2016a). Dataset from: Visual landmarks sharpen grid cell metric and confer context specificity to neurons of the medial entorhinal cortex. *Dryad Digital Repository*. <http://dx.doi.org/10.5061/dryad.c261c>
- Pérez-Escobar, J. A., Kornienko, O., Latuske, P., Kohler, L., & Allen, K. (2016b). Visual landmarks sharpen grid cell metric and confer context specificity to neurons of the medial entorhinal cortex. *Elife*, 5, e16937.
- Pérez-Escobar, J. A. (2020). Mathematical Modelling and Teleology in Biology. In *Research in History and Philosophy of Mathematics*, 69-82. Cham: Birkhäuser.

- Pérez-Escobar, J. A. (2022). Showing Mathematical Flies the Way Out of Foundational Bottles: The Later Wittgenstein as a Forerunner of Lakatos and the Philosophy of Mathematical Practice. *KRITERION—Journal of Philosophy*.
- Piccinini, G. and Craver, C. (2011). Integrating psychology and neuroscience: Functional analyses as mechanism sketches. *Synthese* 183(3), 283-311.
- Pinker, S. (2003). *The blank slate: The modern denial of human nature*. Penguin.
- Pollock, E., Desai, N., Wei, X. X., & Balasubramanian, V. (2018). Dynamic self-organized error-correction of grid cells by border cells. *arXiv preprint arXiv:1808.01503*.
- Poulter, S., Hartley, T., & Lever, C. (2018). The neurobiology of mammalian navigation. *Current Biology*, 28(17), R1023-R1042.
- Quine, W. V. (1951). Main trends in recent philosophy: Two dogmas of empiricism. *The philosophical review* 60, 20-43.
- Raichle, M. E. (2009). A brief history of human brain mapping. *Trends in neurosciences*, 32(2), 118-126.
- Ramsey, W. (2020). Defending representation realism. In J. Smortchkova, K. Dolega, T. Schlicht (Eds.), *What are Mental Representations?* (pp. 54-78). New York: Oxford University Press.
- Ranck, J. B. (1984). Head direction cells in the deep layer of dorsal presubiculum in freely moving rats. *Society of Neuroscience Abstracts*, 10, 599.
- Raudies, F., Mingolla, E., & Hasselmo, M. E. (2012). Modeling the influence of optic flow on grid cell firing in the absence of other cues. *Journal of computational neuroscience*, 33(3), 475-493.
- Rodríguez-Domínguez, U., & Caplan, J. B. (2019). A hexagonal Fourier model of grid cells. *Hippocampus*, 29(1), 37-45.
- Royer, S., Zemelman, B. V., Losonczy, A., Kim, J., Chance, F., Magee, J. C., & Buzsáki, G. (2012). Control of timing, rate and bursts of hippocampal place cells by dendritic and somatic inhibition. *Nature neuroscience*, 15(5), 769-775.

- Saleem, A. B., Ayaz, A., Jeffery, K. J., Harris, K. D., & Carandini, M. (2013). Integration of visual motion and locomotion in mouse visual cortex. *Nature neuroscience*, *16*(12), 1864-1869.
- Sargolini, F., Fyhn, M., Hafting, T., McNaughton, B. L., Witter, M. P., Moser, M. B., & Moser, E. I. (2006). Conjunctive representation of position, direction, and velocity in entorhinal cortex. *Science*, *312*(5774), 758-762.
- Savelli, F., Yoganarasimha, D., & Knierim, J. J. (2008). Influence of boundary removal on the spatial representations of the medial entorhinal cortex. *Hippocampus*, *18*(12), 1270-1282.
- Savelli, F., Luck, J. D., & Knierim, J. J. (2017). Framing of grid cells within and beyond navigation boundaries. *Elife*, *6*, e21354.
- Schmitzer-Torbert, N. 1., Jackson, J., Henze, D., Harris, K., & Redish, A. D. (2005). Quantitative measures of cluster quality for use in extracellular recordings. *Neuroscience*, *131*(1), 1-11.
- Skaggs, W. E., Knierim, J. J., Kudrimoti, H. S., & McNaughton, B. L. (1995). A model of the neural basis of the rat's sense of direction. In *Advances in neural information processing systems 7: Proceedings of the 1994 conference*, 173-180. MIT Press.
- Skaggs, W. E., McNaughton, B. L., Wilson, M. A., & Barnes, C. A. (1996). Theta phase precession in hippocampal neuronal populations and the compression of temporal sequences. *Hippocampus*, *6*(2), 149-172.
- Solstad, T., Boccara, C. N., Kropff, E., Moser, M. B., & Moser, E. I. (2008). Representation of geometric borders in the entorhinal cortex. *Science*, *322*(5909), 1865-1868.
- Stensola, H., Stensola, T., Solstad, T., Frøland, K., Moser, M. B., & Moser, E. I. (2012). The entorhinal grid map is discretized. *Nature*, *492*(7427), 72-78.
- Stensola, T., Stensola, H., Moser, M. B., & Moser, E. I. (2015). Shearing-induced asymmetry in entorhinal grid cells. *Nature*, *518*(7538), 207-212.

- Sullivan, J. A. (2010a). A role for representation in cognitive neurobiology. *Philosophy of Science*, 77(5), 875-887.
- Sullivan, J. A. (2010b). Reconsidering 'spatial memory' and the Morris water maze. *Synthese*, 177(2), 261-283.
- Taube, J. S., Muller, R. U., & Ranck, J. B. (1990a). Head-direction cells recorded from the postsubiculum in freely moving rats. I. Description and quantitative analysis. *Journal of Neuroscience*, 10(2), 420-435.
- Taube, J. S., Muller, R. U., & Ranck, J. B. (1990b). Head-direction cells recorded from the postsubiculum in freely moving rats. II. Effects of environmental manipulations. *Journal of Neuroscience*, 10(2), 436-447.
- Taube, J. S. (1995). Head direction cells recorded in the anterior thalamic nuclei of freely moving rats. *Journal of Neuroscience*, 15(1), 70-86.
- Taube, J. S., & Shinder, M. E. (2020). On the absence or presence of 3D tuned head direction cells in rats: a review and rebuttal. *Journal of Neurophysiology*, 123(5), 1808-1827.
- Tennant, S. A., Fischer, L., Garden, D. L., Gerlei, K. Z., Martinez-Gonzalez, C., McClure, C., ... & Nolan, M. F. (2018). Stellate cells in the medial entorhinal cortex are required for spatial learning. *Cell reports*, 22(5), 1313-1324.
- Tennant, S. A., Clark, H., Hawes, I., Tam, W. K., Hua, J., Yang, W., ... & Nolan, M. F. (2022). Spatial representation by ramping activity of neurons in the retrohippocampal cortex. *Current Biology*, 32(20), 4451-4464.
- Thorndike, E. L. (1898). Animal intelligence: An experimental study of the associative processes in animals. *Psychological Monographs: General and Applied*, 2(4), i-109.
- Thorndike, E. L. (1905). *The elements of psychology*. A. G. Seiler.
- Tolman, E. C., Ritchie, B. F., & Kalish, D. (1946a). Studies in spatial learning. I. Orientation and the short-cut. *Journal of experimental psychology*, 36(1), 13.
- Tolman, E. C., Ritchie, B. F., & Kalish, D. (1946b). Studies in spatial learning. II. Place learning versus response learning. *Journal of experimental psychology*, 36(3), 221.

- Tolman, E. C. (1948). Cognitive maps in rats and men. *Psychological review*, 55(4), 189.
- Valerio, S., & Taube, J. S. (2012). Path integration: how the head direction signal maintains and corrects spatial orientation. *Nature neuroscience*, 15(10), 1445.
- Vandrey, B., Duncan, S., & Ainge, J. A. (2021). Object and object-memory representations across the proximodistal axis of CA1. *Hippocampus*, 31(8), 881-896.
- Wilson, M. A., & McNaughton, B. L. (1993). Dynamics of the hippocampal ensemble code for space. *Science*, 261(5124), 1055-1058.
- Winter, S. S., Clark, B. J., & Taube, J. S. (2015). Disruption of the head direction cell network impairs the parahippocampal grid cell signal. *Science*, 347(6224), 870-874.
- Yoder, R. M., Clark, B. J., Brown, J. E., Lamia, M. V., Valerio, S., Shinder, M. E., & Taube, J. S. (2011). Both visual and idiothetic cues contribute to head direction cell stability during navigation along complex routes. *Journal of Neurophysiology*, 105(6), 2989-3001.
- Yoon, K., Buice, M. A., Barry, C., Hayman, R., Burgess, N., & Fiete, I. R. (2013). Specific evidence of low-dimensional continuous attractor dynamics in grid cells. *Nature neuroscience*, 16(8), 1077-1084.

## 8. PUBLICATIONS

The work presented in this dissertation has been conducted at the Department of Clinical Neurobiology of the Medical Faculty of Heidelberg University and the German Cancer Research Center (DKFZ) under the supervision of Prof. Dr. Hannah Monyer and Dr. Kevin Allen.

Most of the experimental results reported in this thesis, but excluding theoretical reflections, the introductory framing and much of the discussion, have been published as a relatively dense and highly cited article in 2016 in the prestigious journal *eLife*. Therefore, many passages have been quoted verbatim from Pérez-Escobar et al. (2016), of which I hold first authorship, as acknowledged extensively in the main text. As the Author Details and Contribution sections of the paper show, I have been involved in all steps of the research: “Conception and design, Acquisition of data, Analysis and interpretation of data, Drafting or revising the article”. My supervisor’s evaluation further reflects this: The article, however, contains input, suggestions and corrections by the coauthors, especially by my scientific supervisor, Dr. Kevin Allen, who was my *de facto* scientific supervisor/mentor in the above steps. No other publications of mine have been used for the content of this dissertation, except for very brief allusions to my recent work in the discussion.

As for the copyright of the publication: I retain reproduction rights, including the context of this dissertation. This is because the publication is in Open Access and under a Creative Commons Attribution License (CC BY 4.0) that allows me to “Share – copy and redistribute the material in any medium or format, and Adapt – remix, transform, and build upon the material for any purpose, even commercially”. This is also explicit in the paper itself: “This article is distributed under the terms of the Creative Commons Attribution License, which permits unrestricted use and redistribution provided that the original author and source are credited”.

Publication:

Pérez-Escobar, J. A., Kornienko, O., Latuske, P., Kohler, L., & Allen, K. (2016). Visual landmarks sharpen grid cell metric and confer context specificity to neurons of the medial entorhinal cortex. *Elife*, 5, e16937.

## ACKNOWLEDGEMENTS

This work would not have been possible without the help and support of many people, in both academic and personal contexts. This is the case for several reasons. On one hand, there are academic reasons; in fact, it is well known that an appropriate academic supervision is one of the main ingredients of a successful dissertation. But on the other hand, there is much more going on during the long years that the typical PhD takes, especially for students that leave their hometown for a completely new living environment. That was my case, but this short description shall suffice here: its purpose is to frame the acknowledgements that follow.

First of all, I would like to thank Dr. Kevin Allen, my main scientific supervisor, for the close guidance and support he has offered me ever since the moment he gave me the chance to work in his (by then recently established) research group. Not only he was involved and available academically, but also, with immense patience and understanding, tried to engage and motivate me during difficult times. Some superficial counterfactual reasoning is enough to suggest that, had his dedication been lesser, I probably would not find myself writing these words.

Second, I am grateful to my formal Doktormutter, for all the exchanges that we had (where she shared her wisdom) and the integration in her bigger team (which, via seminars and other meetings, formal and informal, provided me with a broader overview of neuroscientific research). I am also thankful to her for agreeing to be the first referee of this dissertation, and everything that this implies.

I cannot forget about the “in vivos”, the group of colleagues doing in vivo research, all of which shared an office (this fact may sound strange these days). Some of them are Dr. Patrick Latuske, Laura Kohler, Martin Jendrika, and Dr. Olga Kornienko, who together with me, comprised Dr. Kevin Allen’s cozy group. Other “in vivos”, like Dr. Oana Toader, and Dr. Mihai Ancau, were particularly close to us. They all helped both in the lab and outside.

I must also mention some people outside the Department of Clinical Neurobiology. Concretely, I am grateful for Prof. Dr. Wolfgang Eckart’s willingness to share his knowledge on the history of electrophysiology with me. Prof. Eckart, who I had the

privilege to meet before his recent passing away, left an intellectual footprint that will never be forgotten. I also want to thank Prof. Dr. Thomas Fuchs for inviting me to participate in inspiring discussions in his group seminar and introducing me to the topic of embodied cognition.

## EIDESSTATTLICHE VERSICHERUNG (AFFIDAVIT)

1. Bei der eingereichten Dissertation zu dem Thema

Context-specificity of spatially selective neurons in the medial entorhinal cortex

handelt es sich um meine eigenständig erbrachte Leistung.

2. Ich habe nur die angegebenen Quellen und Hilfsmittel benutzt und mich keiner unzulässigen Hilfe Dritter bedient. Insbesondere habe ich wörtlich oder sinngemäß aus anderen Werken übernommene Inhalte als solche kenntlich gemacht.

3. Die Arbeit oder Teile davon habe ich wie folgt / bislang nicht an einer Hochschule des In- oder Auslands als Bestandteil einer Prüfungs- oder Qualifikationsleistung vorgelegt.

4. Die Richtigkeit der vorstehenden Erklärungen bestätige ich.

5. Die Bedeutung der eidesstattlichen Versicherung und die strafrechtlichen Folgen einer unrichtigen oder unvollständigen eidesstattlichen Versicherung sind mir bekannt.

Ich versichere an Eides statt, dass ich nach bestem Wissen die reine Wahrheit erkläre und nichts verschwiegen habe.

Ort und Datum

Unterschrift

**Heidelberg, 05.05.2023**